Uniform biodegradable fiber-like micelles and block comicelles via “living” crystallization-driven self-assembly of poly(L-lactide) block copolymers

He, Yunxiang; Eloi, Jean-Charles; Harniman, Robert L ; Richardson, Robert M.; Whittell, George R; Mathers, Robert T.; Dove, Andrew; O'Reilly, Rachel; Manners, Ian

DOI:
10.1021/jacs.9b09885

License:
Other (please specify with Rights Statement)

Document Version
Peer reviewed version

Citation for published version (Harvard):
He, Y, Eloi, J-C, Harniman, RL, Richardson, RM, Whittell, GR, Mathers, RT, Dove, A, O'Reilly, R & Manners, I 2019, 'Uniform biodegradable fiber-like micelles and block comicelles via “living” crystallization-driven self-assembly of poly(-lactide) block copolymers : the importance of reducing unimer self-nucleation via hydrogen bond disruption', *Journal of the American Chemical Society*, vol. 141, no. 48, pp. 19088-19098. https://doi.org/10.1021/jacs.9b09885

Supporting Information of

Uniform Biodegradable Fiber-Like Micelles and Block Co-micelles via 'Living' Crystallization-Driven Self-Assembly of Poly(*L*-lactide) Block Copolymers: The Importance of Reducing Unimer Self-Nucleation via Hydrogen Bond Disruption

Yunxiang He,[1] Jean-Charles Eloi,[1] Robert L. Harniman,[1] Robert M. Richardson,[2] George R. Whittell,[1] Robert T. Mathers,[3] Andrew P. Dove,[4*] Rachel K. O'Reilly,[4*] and Ian Manners[1,5*]

[1]School of Chemistry, University of Bristol, Bristol BS8 1TS, UK

[2]School of Physics, University of Bristol, Tyndall Avenue, Bristol, BS8 1TL, UK

[3]Department of Chemistry, Pennsylvania State University, New Kensington, PA 15068, USA

[4]School of Chemistry, University of Birmingham, Edgbaston, Birmingham, B15 2TT, UK

[5]Department of Chemistry, University of Victoria, Victoria, BC V8W 3V6, Canada

[*]To whom correspondence should be addressed:

a.dove@bham.ac.uk

r.oreilly@bham.ac.uk

imanners@uvic.ca

Materials and Methods

All reactions were carried out in an MBraun MB150B-G glove box under nitrogen atmosphere or using standard Schlenk line techniques. Solvents for self-assembly were purchased at HPLC grade and filtered through a PTFE membrane with pore size of 450 nm. Solvents for reactions were obtained from a Grubbs type solvent purification system. All reagents and solvents were purchased from Sigma-Aldrich (UK), Acros, Fluka, Fisher Chemical and Alfa Aesar, and used as received unless otherwise noted. *L*-Lactide were purified by azeotropic distillation or recrystallization respectively from toluene, followed by drying at 50 °C under reduced pressure over night prior to use. *N*-Isopropylacrylamide (NIPAm) was recrystallized twice from methanol before use. 2,2′-Azobis(2-methylpropionitrile) (AIBN) was recrystallized twice from methanol and stored in the dark at 4 °C. 2-Vinylpyridine (2VP) was passed through a basic aluminium oxide column before use. DBU were dried over CaH_2 and distilled under vacuum before use.

Matrix-assisted laser desorption/ionization time of flight (MALDI-TOF) mass spectrometry measurements were performed using a Bruker Ultraflextreme running in linear mode. Samples were prepared using a *trans*-2-[3-(4-*tert*-butylphenyl)-2-methyl-2-propenylidene]malononitrile matrix (20 mg/mL in THF) and the polymer sample (2 mg/mL in THF), mixed in a 10:1 (*v*/*v*) ratio. Approximately 1 μL of the mixed solution was deposited onto a stainless steel sample plate and allowed to dry in air.

^{1}H and ^{13}C NMR spectra were obtained using a Varian 400 MHz spectrometer with $CDCl_3$ (^{1}H NMR: δ = 7.26 ppm; ^{13}C NMR δ = 77.16 ppm) as solvents and integrations of all peaks were against to TMSCl standard in NMR solvents. DOSY NMR spectra were obtained using a Varian 500 MHz spectrometer with $CDCl_3$ as solvents.

Infrared spectra (IR) were recorded on a Perkin Elmer Spectrum One Fourier Transform Infrared Spectrometer (FT-IR).

Thermogravimetric analysis (TGA) was performed on a TA Instruments Q100 calorimeter at a scan rate of 10 °C/min under nitrogen.

Gel Permeation Chromatography (GPC) was conducted on a Viscotek VE2001 GPCmax chromatograph equipped with a refractive indices (RI) and a UV detector array. *n*-Bu_4NBr/THF (0.1 w/w %) was used as the eluent, with the flow rate set at 1 mL/min. The columns used were of grade GP5000HHR followed by GP2500HHR (Viscotek) at a constant

temperature of 30 °C. The calibration of RI detector was carried out using polystyrene standards (Viscotek). Samples were prepared at 2 mg/mL in eluent and filtered through a Ministart SRP 15 filter (polytetrafluorethylene membrane, pore size = 0.45 μm).

Dynamic light scattering (DLS) was employed to determine the size of micelles formed in selective solvents. The measurements were performed at 25 °C on a Malvern Instruments Zetasizer Nano S using a 5 mW He−Ne laser (633 nm) and a detector oriented at 173°. Samples (1 mL) were measured in an optical glass cuvette (10.0 mm path length) with a concentration of 0.05 mg/mL. The results of DLS studies are reported as apparent hydrodynamic radii ($R_{h,app}$), acknowledging that the particles have been modelled as spheres in the experiments conducted.

Transmission electron microscopy **(**TEM) images were obtained on a JEOL 1400 microscope with a SIS MegaViewIII digital camera, which was operated at 120 kV. Selected area electron diffraction (SAED) data and scanning transmission election microscopy (STEM) images were obtained on a JEOL JEM-2100F field emission TEM equipped with an Oxford Instruments X-Max 80 mm2 X-ray detector WITH Aztec software from Oxford Instruments. STEM was operated in high angle annular dark field imaging (HAADF) mode. Samples were prepared by drop casting 4 μL of the micelle solution onto a carbon coated copper grid. Copper grids (400 mesh) were purchased from Agar Scientific and carbon films were prepared on mica sheets by carbon sputtering with an Agar TEM Turbo Carbon Coater. The carbon films were deposited onto the copper grids by floatation on water and the carbon coated grids were allowed to dry in air. For TEM images, samples were stained with uranyl acetate solution (2% wt in EtOH). For STEM and SAED data, no staining was applied.

For micelle contour lengths analysis, ca. 200 micelles in several images were traced manually using the ImageJ software package developed at the US National Institute of Health. The number average micelle length (L_n) and weight average micelle length (L_w) were calculated using eq. S1 from measurements of the contour lengths (L_i) of individual micelles, where N_i is the number of micelles of length L_i, and n is the number of micelles examined in each sample. The distribution of micelle lengths is characterized by both L_w/L_n and the ratio of standard deviation/L_n (σ/L_n).

$$L_n = \frac{\sum_{i=1}^{n} N_i L_i}{\sum_{i=1}^{n} Ni} \qquad L_w = \frac{\sum_{i=1}^{n} N_i L_i^2}{\sum_{i=1}^{n} NiLi} \qquad \text{(eq.S1)}$$

Atomic force microscopy (AFM) analyses were performed in ambient conditions using a Bruker Multimode VIII atomic force microscope equipped with a ScanAsyst-HR fast scanning module and a ScanAsyst-Air-HR probe (tip radius, 2 nm), utilising peak force feedback control. Samples for AFM were prepared by drop casting 6 μL of micelle colloidal solution onto freshly cleaved mica before drying with a gentle stream of nitrogen.

X-ray scattering measurements (small- and wide-angle, SAXS and WAXS, respectively) were performed in transmission geometry using a Ganesha small angle X-ray scattering apparatus (SAXSLAB, Denmark). Solution samples were sealed into 1.5 mm diameter quartz capillary tubes (Capillary Tube Supplies, Cornwall, UK) and solid-state samples were drop cast onto mica or Kapton film (4,4'-oxydiphenylene-pyromellitimide, DuPont). The capillary or film was then secured in position, perpendicular to the X-ray beam and the detector was positioned at a distance of 1050 mm and 100 mm for the SAXS and WAXS measurements respectively. All measurements were recorded after evacuating the chamber to reduce air scattering. All the SAXS data was analyzed after applying corrections for the scattering from the solvents and the empty capillary tube. SAXGUI (from SAXSLAB) was used for empty cell correction and SIMPLE SUBTRACT (in-house) for solvent.

Computation of ctanol-water partition coefficient normalized by the Connolly surface area ($LogP_{oct}$/SA) values. $LogP_{oct}$/SA values were calculated with a similar reported method.[1] $LogP_{oct}$/SA values were calculated with the ALogP98 method in Materials Studio 2019. The surface area was calculated after minimizing the energy of the solvents with the Forcite Molecular Dynamics module in Materials Studio 2019.

Synthesis procedures

Synthesis of 4-cyano-4-(((phenethylthio)carbonothioyl)thio)pentanoic acid (CTA-COOH). Following previously reported procedures,[2-3] in an oven-dried round bottom flask, 2-Phenylethanethiol (4.0 mL, 29.86 mmol) was added dropwise to a stirred suspension of K_3PO_4 (8.0 g, 37.69 mmol) in acetone (20 mL) and stirring for 1 h. CS_2 (5.5 mL, 91.45 mmol) was added and the solution turned bright yellow. After stirring for 16 h, the suspension was filtered, and the cake was washed with acetone (2 x 20 mL). After removing the solvents from the filtrate under reduced pressure, the resulting yellow solid was suspended in diethyl ether (100 mL). Solid iodine (3.2 g, 12.61 mmol) was gradually added and then stirred at room temperature for 1 h, and the insoluble white precipitate was removed by filtration. The yellow-brown filtrate was washed with an aqueous solution of sodium thiosulfate, dried over

magnesium sulfate, and then evaporated to yield yellow solid. 4,4′-azobis(4-cyanopentanoic acid) (ACVA) (5.1 g, 17.90 mmol) was added to a solution of the solid in ethyl acetate (50 mL). The solution was degassed by nitrogen bubbling for 30 min and heated at reflux under nitrogen for 16 h. After removal of the solvents under reduced pressure, the crude product was washed with water (5 × 100 mL). The organic phase was concentrated and purified by silica chromatography using a mixed eluent (hexane:ethyl acetate = 4:1, gradually increasing to 1:1) to afford CTA-COOH as an orange oil (4.3 g, 44%). ^{1}H NMR (400 MHz, $CDCl_3$, 298 K): δ (ppm) 7.4-7.2 (m, 5H, Ph), 3.60 (t, 2H, $PhCH_2C\underline{H_2}$), 3.00 (t, 2H, $PhC\underline{H_2}$), 2.70 (t, 2H, $C\underline{H_2}COOH$), 2.6-2.4 (m, 2H, $CNCC\underline{H_2}$), 1.90 (s, 3H, CH_3). ^{13}C NMR (125 MHz, $CDCl_3$, 298 K): δ (ppm) 216.5 ($\underline{C}$=S), 177.2 ($\underline{C}$=O), 139.2, 128.9, 128.6, and 126.9 (Ph), 118.9 (CN), 46.4 ($\underline{C}CN$), 38.1 ($\underline{C}H_2CS$), 34.2 ($Ph\underline{C}H_2$), 33.6 ($CN\underline{C}CH_2$), 29.6 ($\underline{C}H_2COOH$), 24.9 ($\underline{C}H_3$).

Synthesis of 6-hydroxyhexyl 4-cyano-4(((phenethylthio)carbonothioyl)thio)pentanoate (CTA-OH). In an oven-dried Schlenk flask, CTA-COOH (1.0 g, 3.24 mmol) and 1,6-hexanediol (3.0 g, 25.92 mmol) were dissolved in dry $CHCl_3$ (50 mL). EDC·HCl (0.95 g, 4.87 mmol) and DMAP (59 mg, 0.487 mmol) were dissolved in dry $CHCl_3$ (15 mL) in another oven-dried Schlenk flask at ambient temperature, followed by adding into the reaction flask via a syringe. The reaction mixture was stirred under reflux for 48 h, filtered and concentrated to yield orange oil residue. The crude product was purified by silica chromatography (hexane: ethyl acetate = 3:1 as eluent) to afford CTA-OH as an orange oil (870 mg, 61%). ^{1}H NMR (400 MHz, $CDCl_3$, 298 K): δ (ppm) 7.4-7.2 (m, 5H, Ph), 4.12 (t, 2H, $COOC\underline{H_2}$), 3.66 (t, 2H, $C\underline{H_2}OH$), 3.59 (t, 2H, $PhC\underline{H_2}CH_2$), 3.00 (t, 2H, Ph-$C\underline{H_2}$), 2.64 (t, 2H, $C\underline{H_2}$-COOH), 2.6-2.4 (m, 2H, CN-C-$C\underline{H_2}$), 1.90 (s, 3H, $C\underline{H_3}$), 1.7-1.4 (m, 8H, $C\underline{H_2}C\underline{H_2}C\underline{H_2}C\underline{H_2}CH_2OH$). ^{13}C NMR (125 MHz, $CDCl_3$, 298 K): δ (ppm) 216.5 (C=S), 171.6 (C=O), 139.2, 128.9, 128.6, and 126.9 (Ph), 118.9 (CN), 65.3 ($COO\underline{C}H_2$), 62.9 ($\underline{C}H_2OH$), 46.4 ($\underline{C}CN$), 38.1 ($\underline{C}H_2CS$), 34.2 ($Ph\underline{C}H_2$), 34.1 ($CN\underline{C}CH_2$), 32.7 ($\underline{C}H_2CH_2OH$), 30.6 ($\underline{C}H_2COOH$), 28.7 ($COOCH_2\underline{C}H_2$), 25.8 ($COOCH_2CH_2\underline{C}H_2$), 25.5 ($\underline{C}H_2CH_2CH_2OH$), 24.9 ($\underline{C}H_3$).

Synthesis of $PLLA_{47}$. In a nitrogen-filled glove box, solutions of DBU (11.2 uL, 0.18 mmol) and CTA-OH (28 mg, 0.062 mmol) in dry DCM (2 mL) were added to solution of *L*-lactide (400 mg, 2.78 mmol) in dry DCM (1mL). After stirring for 1 min at room temperature, the solution was quenched with benzoic acid and stirred for 30 min. After removed from the glove box, the reaction solution was precipitated three times into MeOH and collected by centrifugation. The Polymer was further dried in a vacuum oven for 16 h before

characterization (367 mg, 92%). ^{1}H NMR (400 MHz, $CDCl_3$): δ (ppm) 5.17 (q, 102H, C<u>H</u>CH_3), 1.57 (d, 306H, CHC<u>H</u>$_3$). M_n (NMR): 7698 g·mol^{-1}. MALDI: m/z = 7232, DP_n = 47. GPC (*n*-Bu_4NBr/THF, PS standard): M_n = 9800 g·mol^{-1}, $Đ_m$ = 1.09. ν_{max} (neat)/cm^{-1}: 3000-2880 (C-H); 1755, 1044 (C=O); 1456 (CH_3); 1210-1163 (C(O)-O); 1088 (C-O).

Synthesis of PLLA$_{47}$-*b*-PNIPAm$_{267}$. PLLA$_{47}$ (100 mg, 0.015 mmol), NIPAm (355 mg, 3.2 mmol) and AIBN (0.47 mg, 0.003 mmol) were dissolved in 1,4-dioxane (3 mL) in a Schlenk flask. The solution was then freeze-pump-thawed four times and heated for 3.5 h at 70 °C. The reaction was quenched by immersion of the ampoule in liquid nitrogen and the block copolymer was precipitated in hexane three times, followed by drying under vacuum (403 mg, 88%). DP of PNIPAm was confirmed by ^{1}H NMR spectrum based on PLLA DP according to MALDI-TOF spectrometry. ^{1}H NMR (400 MHz, $CDCl_3$): δ (ppm) 7.0-5.6 (br, 244H, N<u>H</u>-CH-$(CH_3)_2$), 5.16 (q, 94H, C<u>H</u>(CH_3) from PLLA), 4.00 (br, 267H, NH-C<u>H</u>-$(CH_3)_2$ from PNIPAm), 2.3-0.7 (3673 H, m, C<u>H</u>$_3$ from PNIPAm, CH(C<u>H</u>$_3$) from PLLA, C<u>H</u>C<u>H</u>$_2$ from PNIPAm). GPC (*n*-Bu_4NBr/THF, PS standard): M_n = 180,600 g·mol^{-1}, $Đ_m$ = 1.11. ν_{max} (neat)/cm^{-1}: 3510-3313 (N-H); 3000-2880 (C-H); 1755 (C=O); 1644 (NH-C=O); 1458 (CH_3); 1386-1367 (C-H), 1276-1185 (C-O); 1130,1088 (C-O).

Synthesis of PLLA$_{47}$-*b*-P2VP$_{503}$. PLLA$_{47}$ (100 mg, 0.015 mmol), 2VP (886 μL, 8.25 mmol) and AIBN (0.47 mg, 0.003 mmol) were dissolved in 1,4-dioxane (2 mL) in a Schlenk flask. The solution was then freeze-pump-thawed four times and heated for 16 h at 70 °C. The reaction was quenched by immersion of the ampoule in liquid nitrogen and the polymer was precipitated in hexane three times, followed by drying under vacuum (403 mg, 88%). DP of P2VP was confirmed by ^{1}H NMR spectrum based on PLLA DP according to MALDI-TOF spectrometry. ^{1}H NMR (400 MHz, $CDCl_3$): δ (ppm) 8.41-8.07 (m, 503H, Ar from P2VP), 7.20-6.30 (m, 1510H, Ar from P2VP), 5.16 (q, 94H, C<u>H</u>(CH_3) from PLLA), 2.28-1.48 (1940H, m, CH(C<u>H</u>$_3$) from PLLA, C<u>H</u>C<u>H</u>$_2$ from P2VP). GPC (*n*-Bu_4NBr/THF, PS standard): M_n = 63,245 g·mol^{-1}, $Đ_m$ = 1.25. ν_{max} (neat)/cm^{-1}: 3000-2880 (C-H); 1755, 1044 (C=O); 1590, 1585 (Ar); 1472, 1433 (Ar-C-N); 1088 (C-O); 745 (Ar).

Self-assembly procedures

All solvent compositions are given as volume ratio (*v*:*v*). All micelle length measurements were carried out on ~200 micelles.

Self-nucleation of PLLA$_{47}$-*b*-PNIPAm$_{267}$. 100 μL of PLLA$_{47}$-*b*-PNIPAm$_{267}$ solution (10 mg/mL in DMSO) was added to a vial with an additional 100 μL of DMSO followed by

slow addition of 1800 μL of EtOH resulting a polymer solution of 0.5 mg/mL. The vial contents were aged at 23 °C for 5 days before TEM characterization. A large amount of non-spherical aggregates and polydisperse micelles was observed by TEM images (Figure S7d). To avoid the formation of spherical aggregates a heating-cooling method was employed. 100 μL of $PLLA_{47}$-*b*-$PNIPAm_{267}$ solution (10 mg/mL in DMSO) was added to a vial with 100 μL DMSO and 1800 μL EtOH resulting a polymer solution of 0.5 mg/mL. The vial was sealed and heated at 70 °C for 4 h, followed by slowly cooling to 23 °C. And the solution was carried on aging for 24 h. The polydisperse fiber-like micelles formed were characterized by TEM.

Self-nucleation of $PLLA_{47}$-*b*-$P2VP_{503}$. 100 μL of $PLLA_{47}$-*b*-$P2VP_{503}$ solution (10 mg/mL in DMSO) was added to a vial with 100 μL DMSO and 1800 μL EtOH resulting a polymer solution of 0.5 mg/mL. The vial was sealed and heated at 70 °C for 4 h, followed by slowly cooling to 23 ^{o}C. And the solution was carried on aging for 24 h. The formed polydisperse fiber-like micelles were characterized by TEM.

Preparation of seed micelles. All seed micelle solutions were prepared by sonication of the polydisperse micelle solutions from self-nucleation of polymer in selective solvents and characterized by TEM.

For $PLLA_{47}$-*b*-$PNIPAm_{267}$ seeds (L_n = 36 nm, L_w/L_n = 1.10, σ/L_n: 0.26): sonication of $PLLA_{47}$-*b*-$PNIPAm_{267}$ polydisperse micelles in DMSO/EtOH (1:9) was carried out for 2 h in a water sonication bath cooled with ice.

For $PLLA_{47}$-*b*-$PNIPAm_{267}$ seeds (L_n = 33 nm, L_w/L_n = 1.13, σ/L_n: 0.38): sonication of $PLLA_{47}$-*b*-$PNIPAm_{267}$ polydisperse micelles in DMSO/EtOH (1:9) was carried out for 2 h in a dry ice/acetone bath with a Ultrasonication probe.

For $PLLA_{47}$-*b*-$P2VP_{503}$ seeds (L_n = 29 nm, L_w/L_n = 1.11, σ/L_n: 0.34): sonication of $PLLA_{47}$-*b*-$PNIPAm_{267}$ polydisperse micelles in DMSO/EtOH (1:9) was carried out for 2 h in a in a water sonication bath cooled with ice.

Seeded-growth of $PLLA_{47}$-*b*-$PNIPAm_{267}$.

For seeded-growth without H-bond disruption reagents: 20 μL (for m_{unimer}:$m_{seed} \leq 10.0$) or 10 μL (for m_{unimer}:$m_{seed} > 10.0$) of seed micelle solution (0.5 mg/mL, DMSO:EtOH = 1:9) was diluted in 400 μL EtOH to which was added $PLLA_{47}$-*b*-$PNIPAm_{267}$ unimer (10 mg/mL in DMSO). The volumes of unimer added in were 2.5, 5, 10, 7.5, 10 and 15 μL corresponds to

unimer-to-seed mass ratios of 2.5, 5, 10, 15, 20 and 30, respectively. And the resulting solution was then manually shaken for 10 s and aged for 5 days at 23 °C before TEM characterization.

For seeded-growth with H-bond disruption reagent: 20 μL (for m_{unimer}:$m_{seed} \leq 10.0$) or 10 μL (for m_{unimer}:$m_{seed} > 10.0$) of seed micelle solution (0.5 mg/mL, DMSO:EtOH = 1:9) was diluted in 400 μL TFE/EtOH with volume ratio of 3:97, 3:97, 5:95, 8:92, 10:90 and 15:85 corresponds to unimer-to-seed mass ratios of 2.5, 5, 10, 15, 20 and 30, respectively, and to which solution was added $PLLA_{47}$-*b*-$PNIPAm_{267}$ unimer (10 mg/mL in DMSO) with volumes of 2.5, 5, 10, 7.5, 10 and 15 μL respectively. And the resulting solution was then manually shaken for 10 s and aged for 5 days at 23 °C before TEM characterization.

Seeded-growth of $PLLA_{47}$-*b*-$PNIPAm_{267}$ for kinetic studies.

Same procedures were adopted with seeded-growth experiments of $PLLA_{47}$-*b*-$PNIPAm_{267}$. After unimer addition, aliquots were taken after samples aged for 1 d, 3 d, and 5 d for TEM characterization.

Seeded-growth of $PLLA_{47}$-*b*-$PNIPAm_{267}$ for solvent effect studies.

10 μL of seed micelle solution (0.5 mg/mL, DMSO:EtOH = 1:9) was diluted in 400 μL solution of EtOH and selected solvents (MeOH, THF, Dioxane, DMF, DMSO, Acetone and TFE) individually with volume ratio of 0.5:9.5, 1:9 and 1.5:8.5, respectively. Similar procedures of unimer addition were adopted with seeded-growth experiments of $PLLA_{47}$-*b*-$PNIPAm_{267}$. And the resulting solution was then manually shaken for 10 s and aged for 5 days at 23 °C before TEM characterization.

Preparation of samples for SAXS analysis.

To obtain quality data from SAXS experiments, micelles were prepared at higher concentrations compare with the method mentioned above. Polydisperse micelles of $PLLA_{47}$-*b*-$PNIPAm_{267}$ was prepared at a polymer concentration of 1 mg/mL by adding 200 μL of unimer solution (10 mg/mL in THF) to 1800 μL of EtOH. THF was employed as the common solvent in this preparation due to the large volatility compared with that of DMSO, which allowing the micelle solutions to be concentrated by applying nitrogen flow and resulting micelles suspended in TFE/EtOH. The solution was heated at 70 °C for 4 hours and slowly cool to 23 °C. The solution was further aged for 5 days and then characterized by TEM. The formed polydisperse micelles were sonicated at -78 °C in a dry ice/acetone bath

for 1 h with a Ultrasonicate probe. TEM images showed that the seed micelles had a L_n (and L_w/L_n) of 36 (1.05) nm. 260 μL seed solution was diluted in 1 mL TFE/EtOH (1:9). To the seed solution, 94 μL of unimer (50 mg/mL in THF) was added and the solution was manually shaken for 10 s. The final solution had a polymer concentration of 4.6 mg/mL. After ageing for 24 h, the micelle was determined a L_n (and L_w/L_n) value of 1040 (1.04) by TEM. The sample with a concentration of 4 mg/mL was prepared by adding 50 μL TFE/EtOH (1:9) to the micelle solution (100 μL). The rest micelle solution was concentrated by applying nitrogen flow to ~120 μL. The concentrated micelle solution had a concentration of 30 mg/mL. Samples with 20 mg/mL was prepared by adding 25 uL TFE/EtOH (1:9) to the concentrated micelle solution (50 μL). The micelle solution prepared for SAXS had been used in other characterizations (AFM, SAED and PXRD).

Seeded-growth of $PLLA_{47}$-*b*-$P2VP_{503}$.

Analogous procedures were adopted to those used for the seeded-growth experiments with $PLLA_{47}$-*b*-$PNIPAm_{267}$ in both EtOH and TFE/EtOH. After the unimer addition, samples were manually shaken for 10 s and aged for 5 days at 23 °C before TEM characterization.

Preparation of pentablock co-micelles

For central block 1 micelles: 20 μL of $PLLA_{47}$-*b*-$PNIPAm_{267}$ seed micelle solution (L_n = 33 nm, 0.5 mg/mL, DMSO/EtOH = 1:9) was diluted in 400 μL TFE/EtOH (1:9) to which was added $PLLA_{47}$-*b*-$PNIPAm_{267}$ unimer (9 μL, 10 mg/mL in DMSO). And the resulting solution was then manually shaken for 10 s and aged for 3 days at 23 °C before TEM characterization.

For triblock 1 co-micelles: $PLLA_{47}$-*b*-$P2VP_{503}$ unimer (3 uL, 10 mg/mL in DMSO) was then added to the central block 1 micelle solution (200 uL). The resulting solution was then manually shaken for 10 s and aged for 3 days at 23 °C before TEM characterization.

For pentablock 1 co-micelles: $PLLA_{47}$-*b*-$PNIPAm_{267}$ unimer (3 μL, 10 mg/mL in DMSO) was added to triblock 1 co-micelle solution (100 uL) (see above). The resulting solution was then manually shaken for 10 s and aged for 3 days at 23 °C before TEM characterization.

For central block 2 micelles: 20 μL of $PLLA_{47}$-*b*-$P2VP_{503}$ seed micelle solution (L_n = 29 nm, 0.5 mg/mL, DMSO/EtOH = 1:9) was diluted in 400 μL TFE/EtOH (1:9) to which was added $PLLA_{47}$-*b*-$P2VP_{503}$ unimer (9 μL, 10 mg/mL in DMSO). And the resulting solution was then manually shaken for 10 s and aged for 3 days at 23 °C before TEM characterization.

For triblock 2 co-micelles: $PLLA_{47}$-*b*-$PNIPAm_{267}$ unimer (5 uL, 10 mg/mL in DMSO) was then added to the central block 2 micelle solution (200 uL) (see above). The resulting solution was then manually shaken for 10 s and aged for 3 days at 23 °C before TEM characterization.

For pentablock 2 co-micelles: $PLLA_{47}$-*b*-$P2VP_{503}$ unimer (5 μL, 10 mg/mL in DMSO) was added to the triblock 2 co-micelle solution (100 uL) (see above). The resulting solution was then manually shaken for 10 s and aged for 3 days at 23 °C before TEM characterization.

Discussion on defects in pentablock comicelles.

Triblock co-micelles and pentablock co-micelles were successfully prepared by alternating seeded-growth of $PLLA_{47}$-*b*-$PNIPAm_{267}$ and $PLLA_{47}$-*b*-$P2VP_{503}$ unimers. One of the features of these block co-micelles was that the grown segments were not equivalent in length as would be expected for a controlled living CDSA process (Figure 9**Error! Reference source not found.**). This is proposed caused by the different addition rates of BCPs with different corona-forming block lengths as previously reported.[4-6] In a typical experiment of preparing triblock co-micelles, the growth of $PLLA_{47}$-*b*-$PNIPAm_{267}$ unimer from $PLLA_{47}$-*b*-$P2VP_{503}$ seed micelles is suggested to be a slow step as a consequence of unfavourable corona-corona interactions between PNIPAm (δ = 24.8 $MPa^{1/2}$) and P2VP (δ = 20.8 $MPa^{1/2}$). Once the first unimer from $PLLA_{47}$-*b*-$PNIPAm_{267}$ has been added in this slow step, further unimers can deposit more rapidly. This might result in different lengths in the newly grown outer segments. In the preparation of pentablock co-micelles, the non-equivalent growth would be amplified by the same reason of switching to a different unimers.

Abbreviation

DCM: dichloromethane; TFE: trifluoroethanol; MeOH: methanol; EtOH: ethanol; DMF: N,N-Dimethylformamide; DMSO: Dimethyl sulfoxide; THF: tetrahydrofuran; Dioxane: 1,4-dioxane; CDSA: crystallization-driven self-assembly; σ: standard deviation.

Supplementary figures

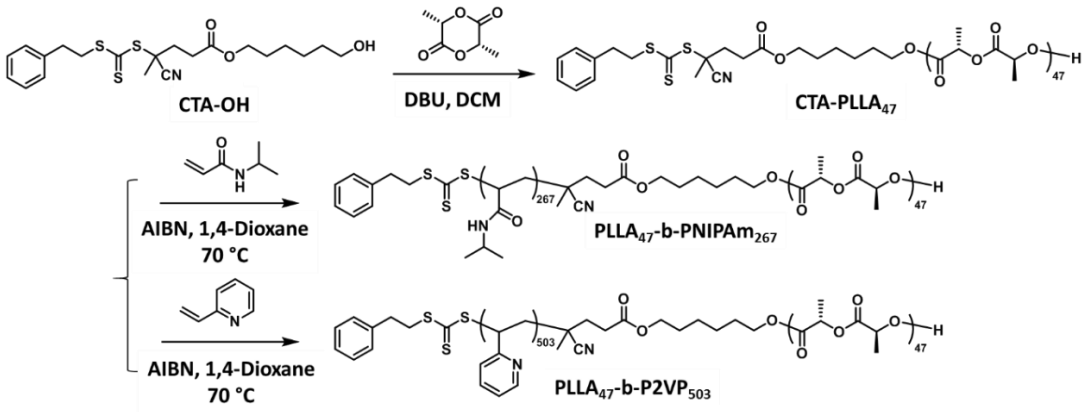

Scheme S1. Synthesis of $PLLA_{47}$-*b*-$PNIPAm_{267}$ and $PLLA_{47}$-*b*-$P2VP_{503}$ diblock copolymers

Table S1. Molar mass characterization of the polymers prepared.

Polymer	M_w (g·mol^{-1})[a]	M_n (kg·mol^{-1})[b]	M_n (kg·mol^{-1})[c]	$Đ_M$[c]	Block ratio (Core:Corona)[b]
$PLLA_{47}$	7232	7.6	10.2	1.09	-
$PLLA_{47}$-*b*-$PNIPAm_{267}$	-	37.4	180[d]	1.11	1:5
$PLLA_{47}$-*b*-$P2VP_{503}$	-	59.7	63.2	1.25	1:10

[a] determined by MALDI;
[b] block ratio (according to degree of polymerization (DP)) determined by ^{1}H NMR spectroscopy;
[c] determined by GPC relative to polystyrene (PS) standards in *n*-Bu_4NBr/THF.
[d] The molar mass estimated by GPC is much larger than that determined by 1H NMR integration. We attribute this to exclusion interactions between the high polar polymer and the low-polarity styrene/divinylbenzene column. Such effects have been previously noted for highly polar polymers[7]

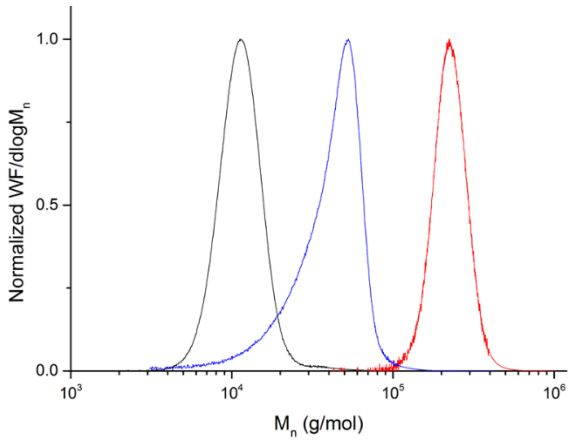

Figure S1. GPC chromatographs (refractive index trace) in n-Bu_4NBr/THF of $PLLA_{47}$ (black, $Đ_m$ = 1.09), $PLLA_{47}$-b-$P2VP_{503}$ (blue, $Đ_m$ = 1.25), $PLLA_{47}$-b-$PNIPAm_{267}$ (red, $Đ_m$ = 1.11).

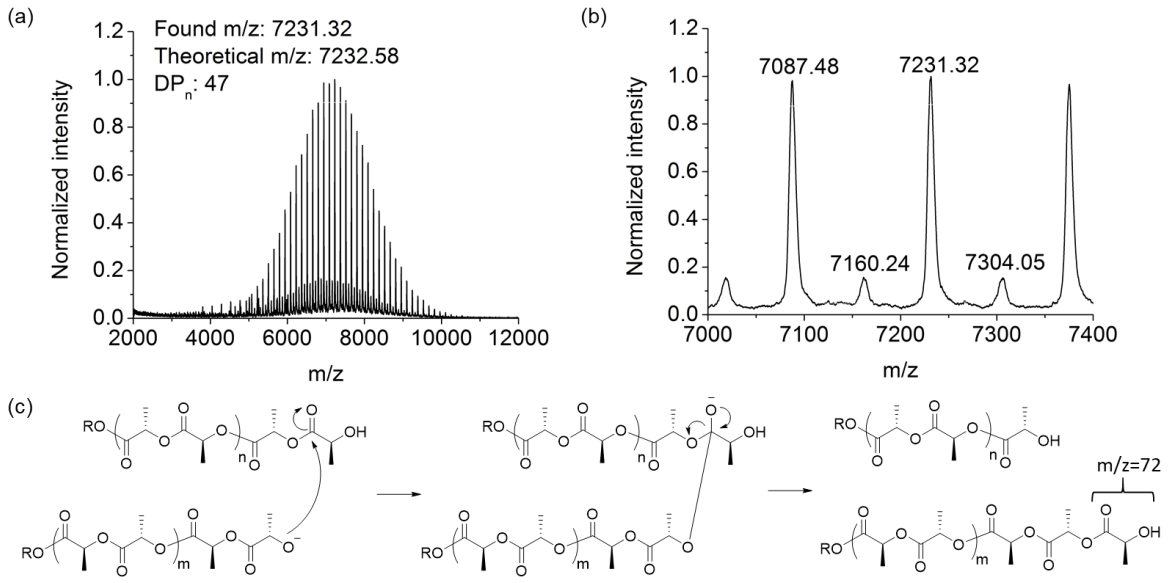

Figure S2. (a) MALDI-TOF MS of CTA-$PLLA_{47}$; (b) Zoom-in MALDI-TOF MS of CTA- $PLLA_{47}$;. (c) Mechanism of transesterification in *L*-lactide polymerization, which corresponds to the minor population possessing a m/z difference of 72 compared with major population in MALDI-TOF MS.

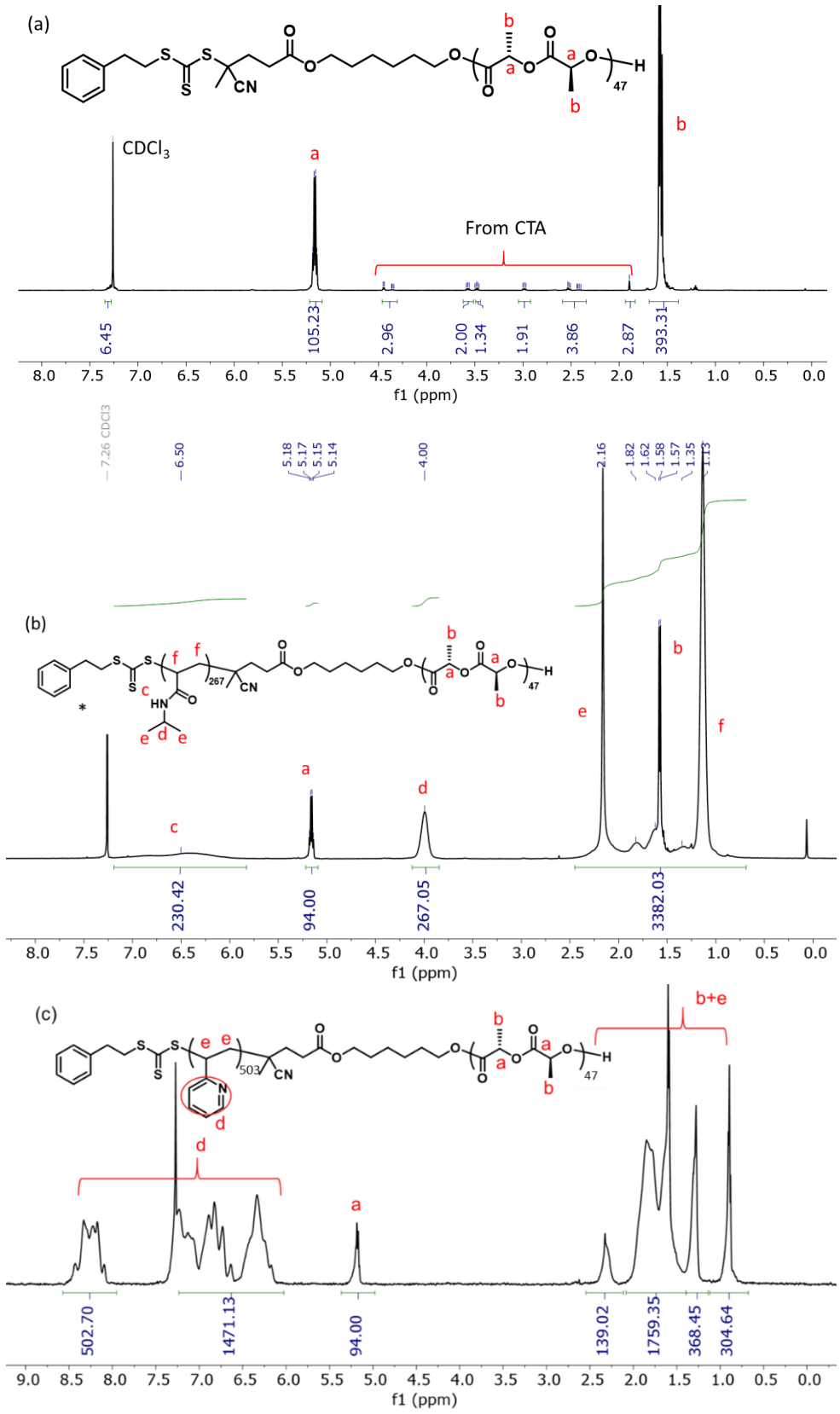

Figure S3. ^{1}H NMR (400 MHz, $CDCl_3$) spectra of (a) CTA-PLLA$_{47}$; (b) PLLA$_{47}$-*b*-PNIPAm$_{267}$ and (c) PLLA$_{47}$-*b*-P2VP$_{503}$.

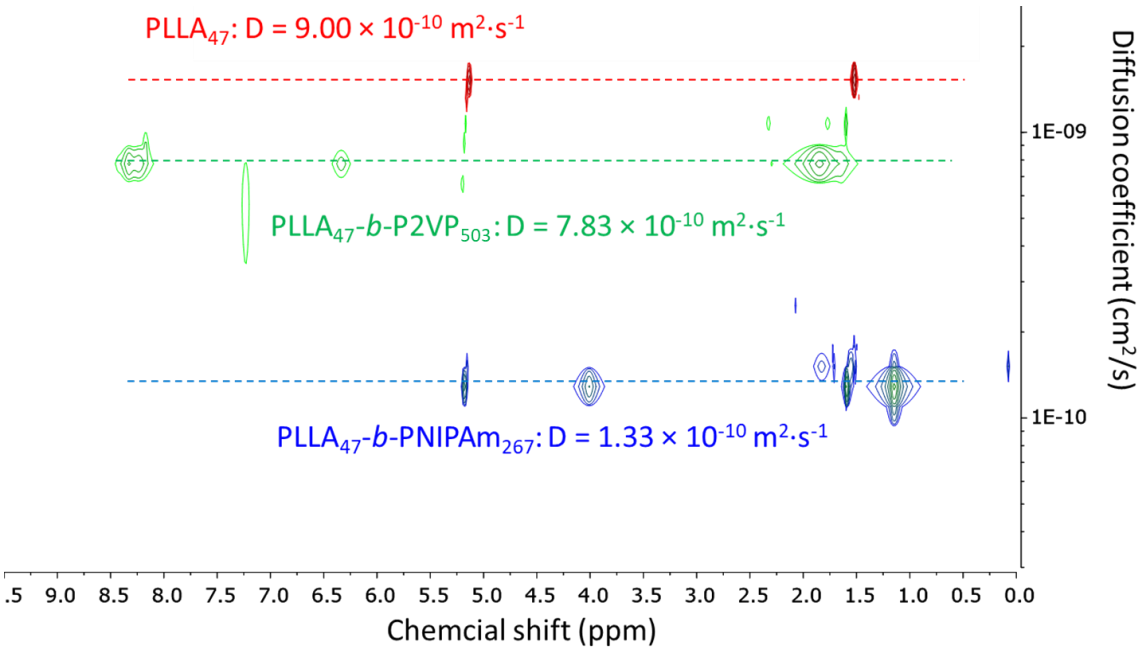

Figure S4. ^{1}H DOSY NMR (500 MHz, $CDCl_3$) spectra of $PLLA_{47}$ (red), $PLLA_{47}$-*b*-$P2VP_{503}$ (green) and $PLLA_{47}$-*b*-$PNIPAm_{267}$ (blue).

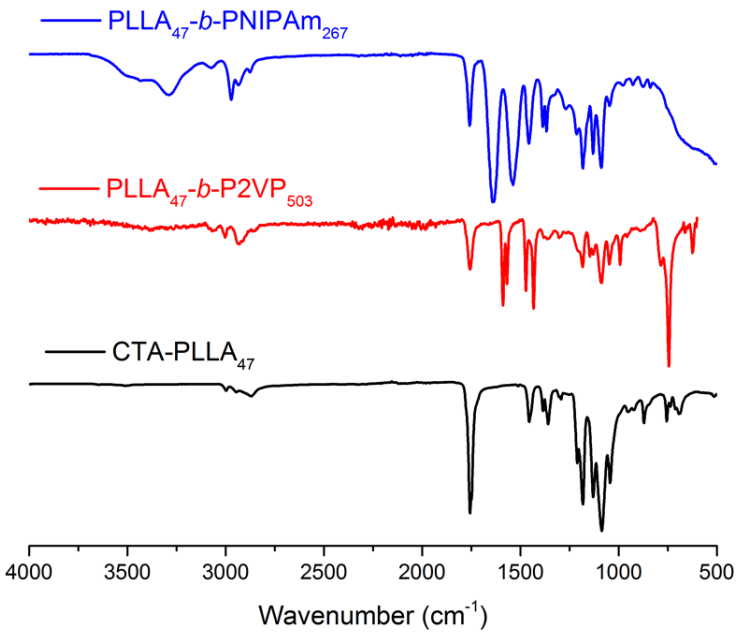

Figure S5. FT-IR characterization of PLLA-containing polymers.

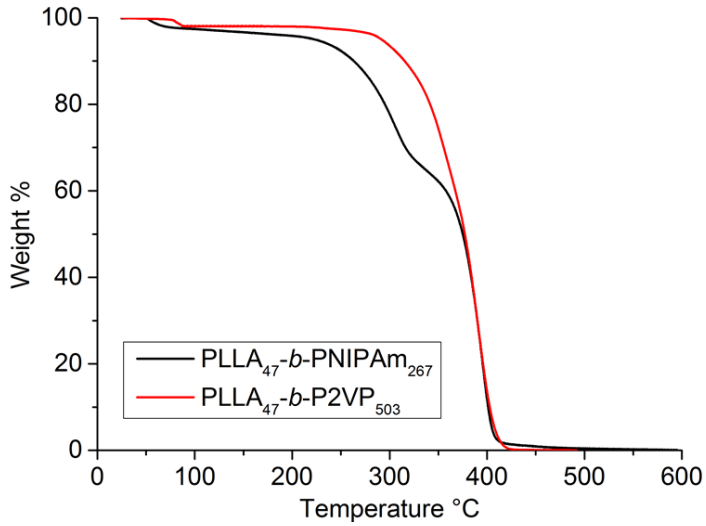

Figure S6. Thermogravimetric analysis (TGA) for $PLLA_{47}$-*b*-$PNIPAm_{267}$ (black) and $PLLA_{47}$-*b*-$P2VP_{503}$ (red). TGA was performed at a scan rate of 10 °C/min under nitrogen.

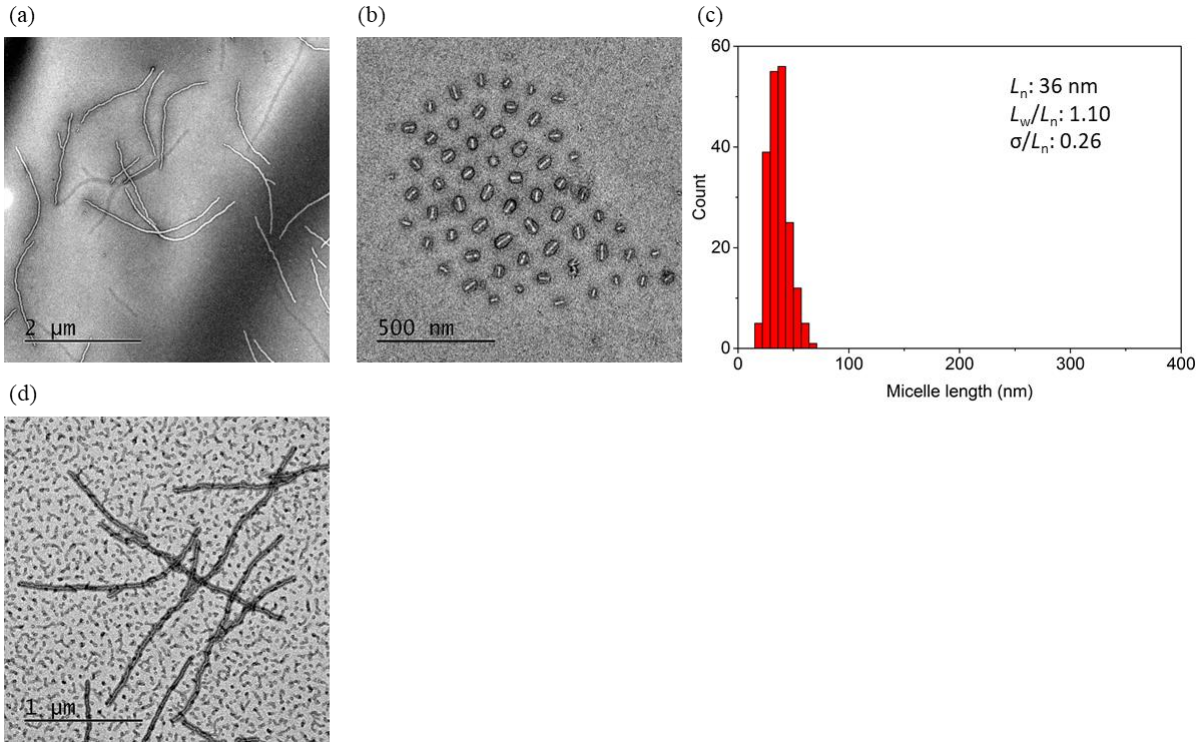

Figure S7. (a) TEM images of polydisperse $PLLA_{47}$-*b*-$PNIPAm_{267}$ micelles prepared by heating the polymer in DMSO/EtOH (1:9) at a concentration of 0.5 mg/mL at 70 °C for 2 h followed by slow cooling down to 23 °C ; (b) TEM images of seeds prepared by sonication of polydisperse micelles at 0 °C for 2 h in a sonic cleaning bath; (c) contour length histogram of measured seeds length, L_n = 36 nm, L_w/L_n = 1.10, σ/L_n: 0.26. TEM samples were stained with a 2 wt% solution of uranyl acetate in EtOH; (d) TEM images of polydisperse $PLLA_{47}$-*b*-$PNIPAm_{267}$ micelles prepared by addition of unimers in DMSO to ethanol and aging at 23 °C for 5 days. A significant amount of non-spherical aggregates was observed.

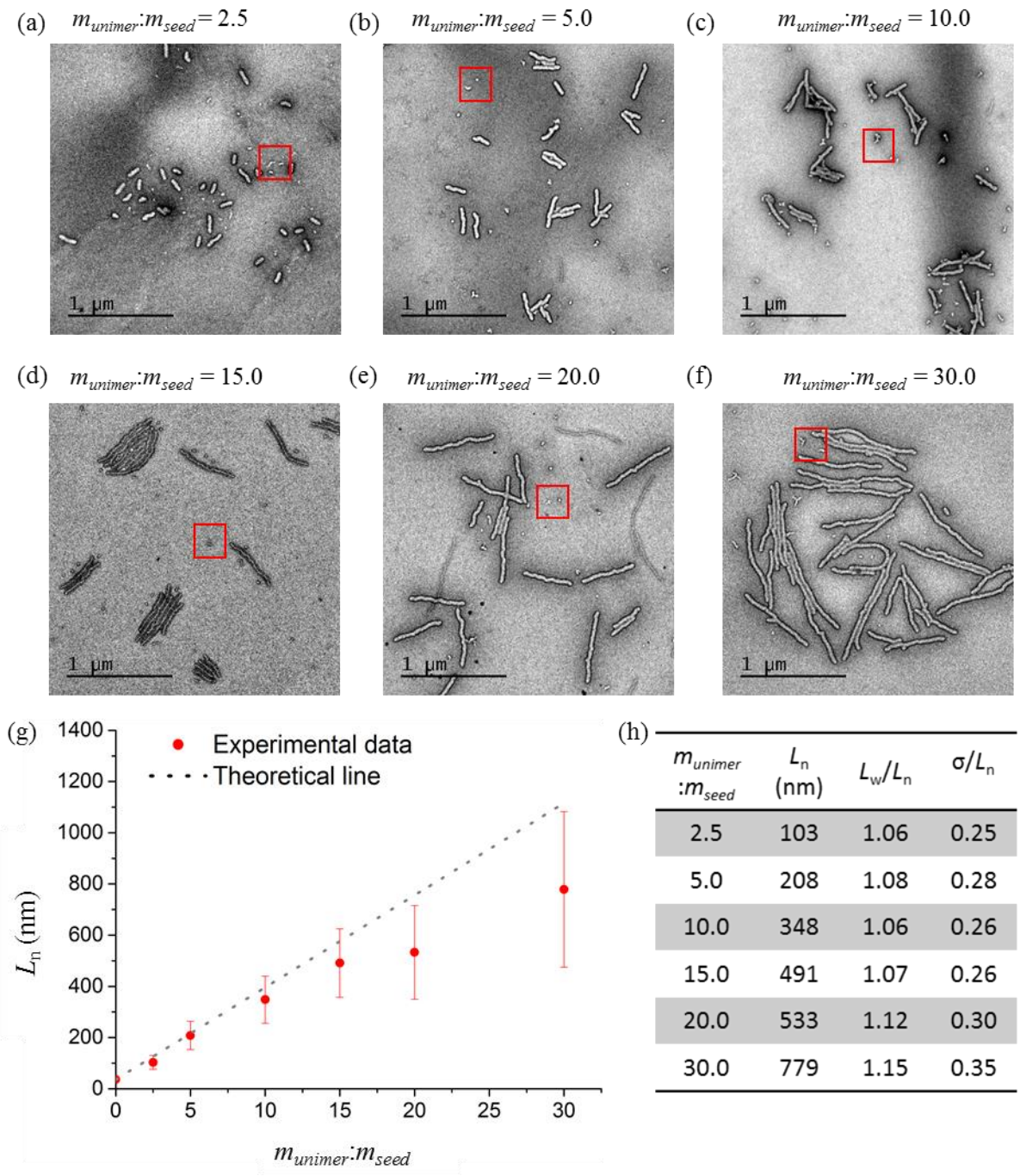

(h)

m_{unimer} :m_{seed}	L_n (nm)	L_w/L_n	σ/L_n
2.5	103	1.06	0.25
5.0	208	1.08	0.28
10.0	348	1.06	0.26
15.0	491	1.07	0.26
20.0	533	1.12	0.30
30.0	779	1.15	0.35

Figure S8. TEM images of samples (aging for 5 days) of elongated $PLLA_{47}$-*b*-$PNIPAm_{267}$ micelles prepared by seeded growth from seed micelles (L_n = 36 nm, L_w/L_n = 1.10, σ/L_n: 0.26) in EtOH after addition of unimers (in DMSO) with unimer-to-seed mass ratios of (a) 2.5, (b) 5.0, (c) 10.0, (d) 15.0, (e) 20.0 and (f) 30.0; (g) plot of micelle number average length verse unimer-to-seed ratios (the error bars represent the standard deviation); (h) measured length data summary. Red rectangles highlight non-spherical particles. TEM samples were stained with a 2 wt% solution of uranyl acetate in EtOH.

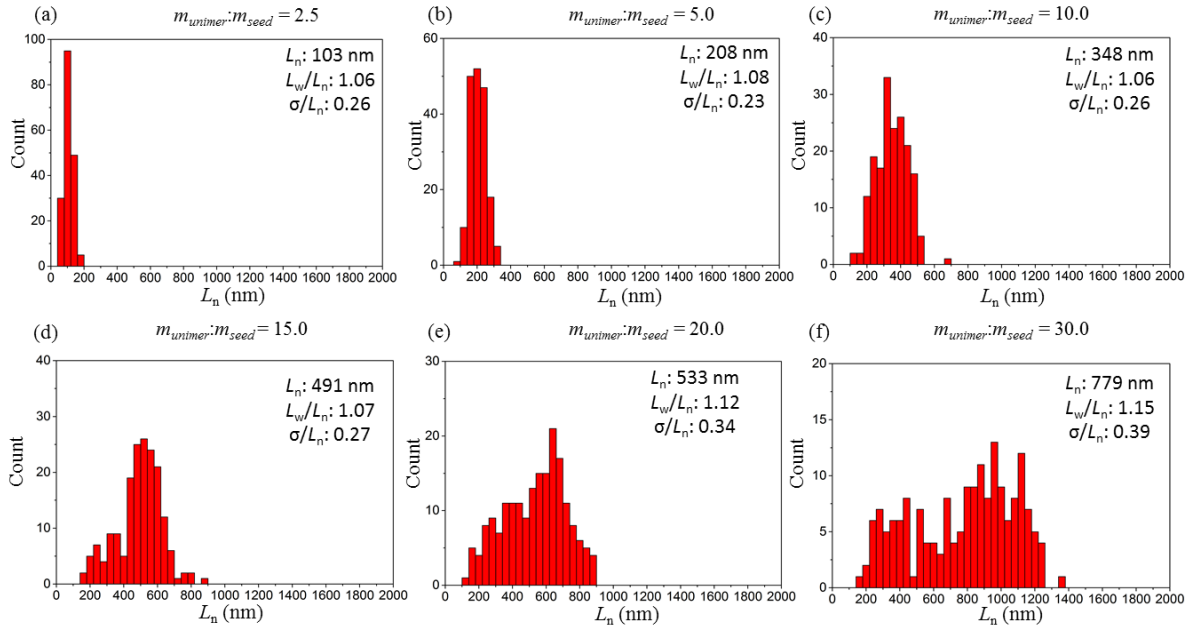

Figure S9. Contour length histogram of 5 days aged elongated PLLA$_{47}$-*b*-PNIPAm$_{267}$ micelles prepared by seeded growth off seed micelles (L_n = 36 nm, L_w/L_n = 1.10, σ/L_n: 0.26) in EtOH after the addition of unimers (in DMSO) with unimer-to-seed mass ratios of (a) 2.5, (b) 5.0, (c) 10.0, (d) 15.0, (e) 20.0 and (f) 30.0.

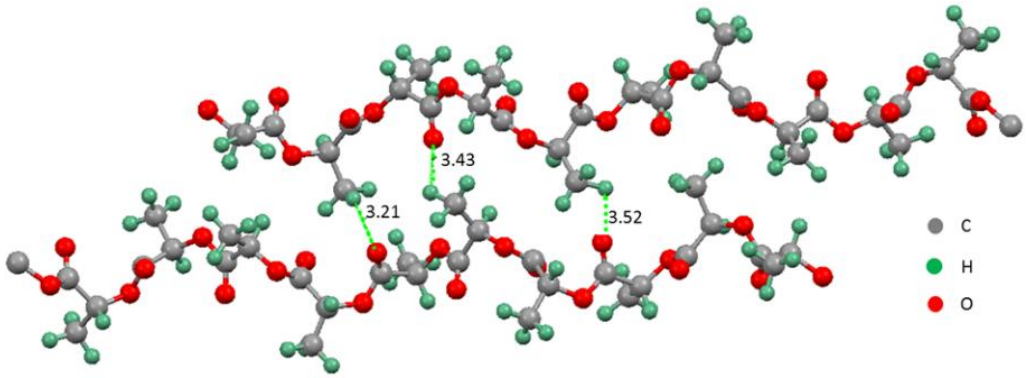

Figure S10. Measurement of O···H distance between two adjacent chains in a model of PLLA α-form crystal cell unit.

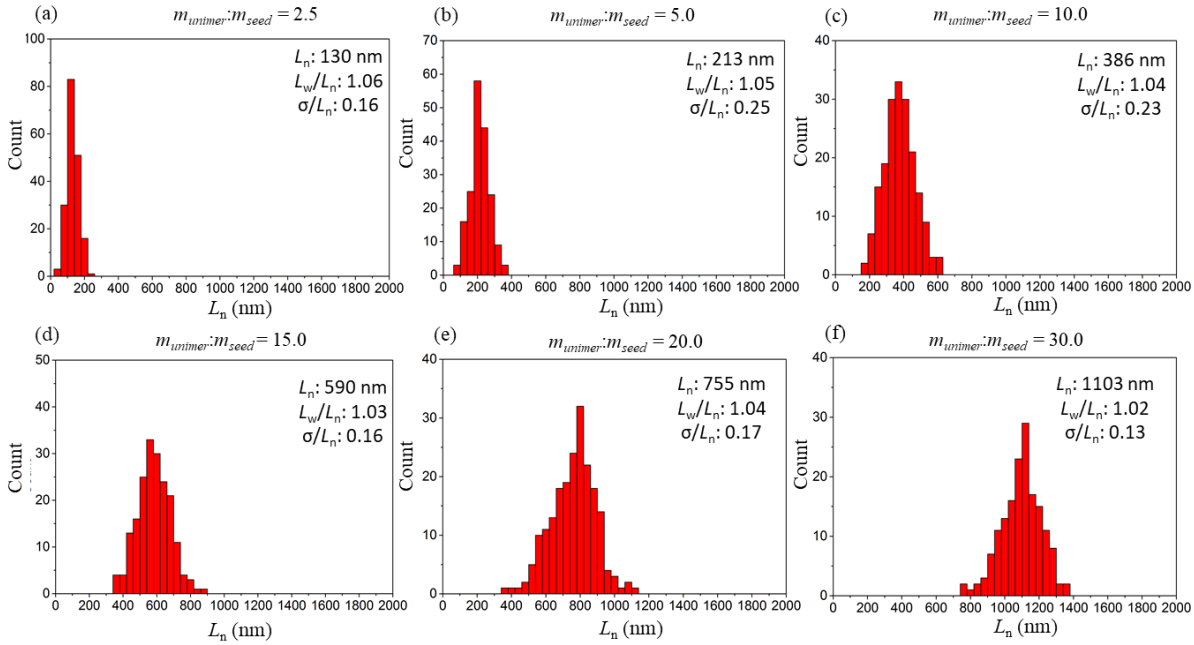

(g)

m_{unimer} :m_{seed}	v_{TFE}: v_{EtOH}	L_n (nm)	L_w/L_n	σ/L_n
2.5	3:97	130	1.09	0.16
5.0	3:97	213	1.06	0.25
10.0	5:95	386	1.05	0.23
15.0	8:92	590	1.03	0.16
20.0	10:90	755	1.03	0.17
30.0	15:85	1103	1.02	0.13

Figure S11. Contour length histogram of 5 days aged uniform $PLLA_{47}$-*b*-$PNIPAm_{267}$ micelles prepared by seeded growth off seed micelles (L_n = 36 nm, L_w/L_n = 1.10, σ/L_n: 0.26) in TFE/EtOH with volume ratios of (a) 3:97, (b) 3:97, (c) 5:95, (d) 8:92, (e) 10:90 and (f) 15:85 after the addition of unimers (in DMSO) with unimer-to-seed mass ratios of (a) 2.5, (b) 5.0, (c) 10.0, (d) 15.0, (e) 20.0 and (f) 30.0, respectively; (g) measured length data summary.

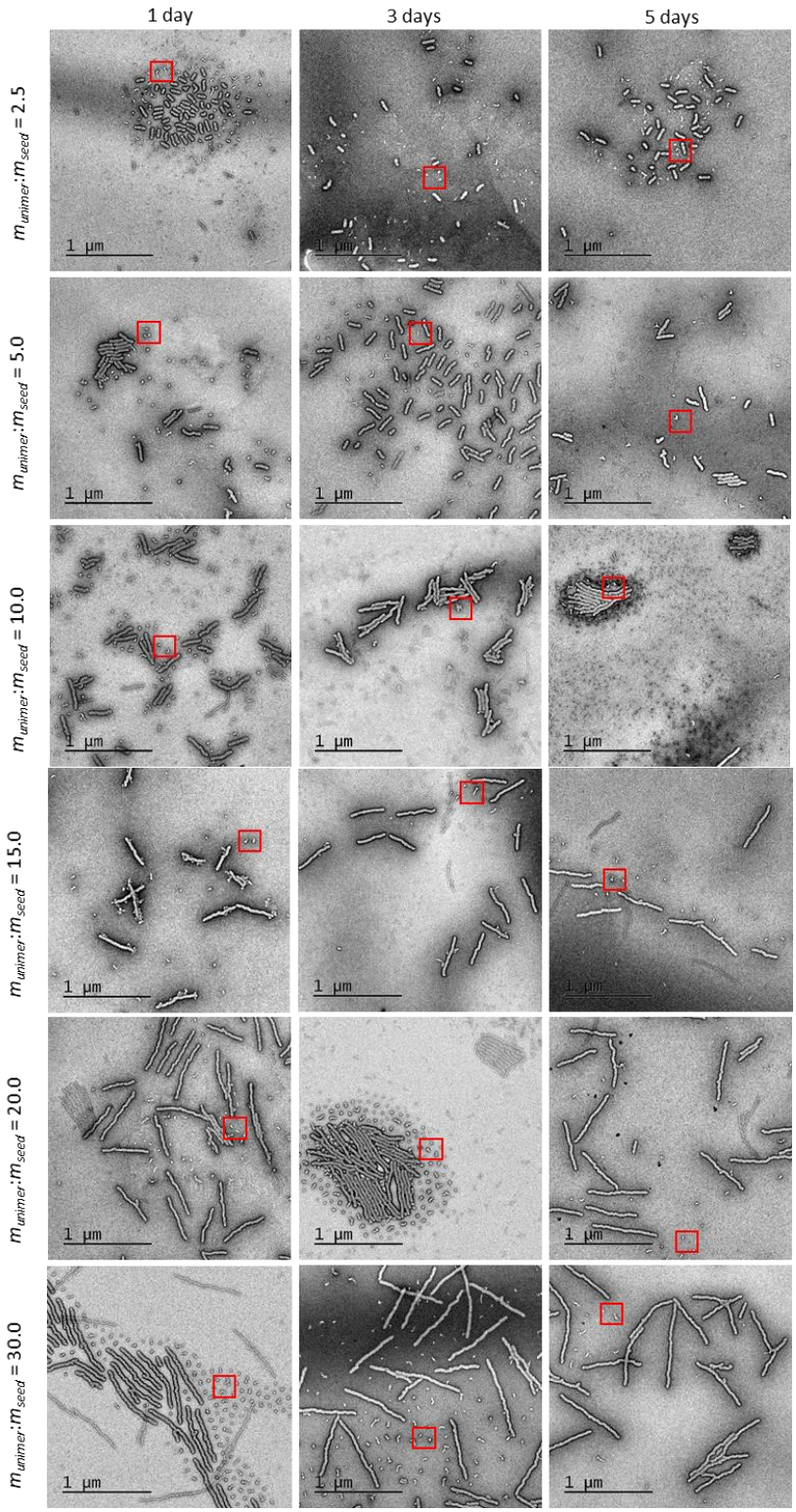

Figure S12. TEM images of elongated $PLLA_{47}$-*b*-$PNIPAm_{267}$ micelles in kinetic studies prepared by seeded growth off seed micelles (L_n = 36 nm, L_w/L_n = 1.10, σ/L_n: 0.26) in EtOH after addition of unimers (in DMSO) with unimer-to-seed mass ratios of 2.5, 5.0, 10.0, 15.0, 20.0 and 30.0; Red rectangles highlight non-spherical particles. TEM samples were stained with a 2 wt% solution of uranyl acetate in EtOH.

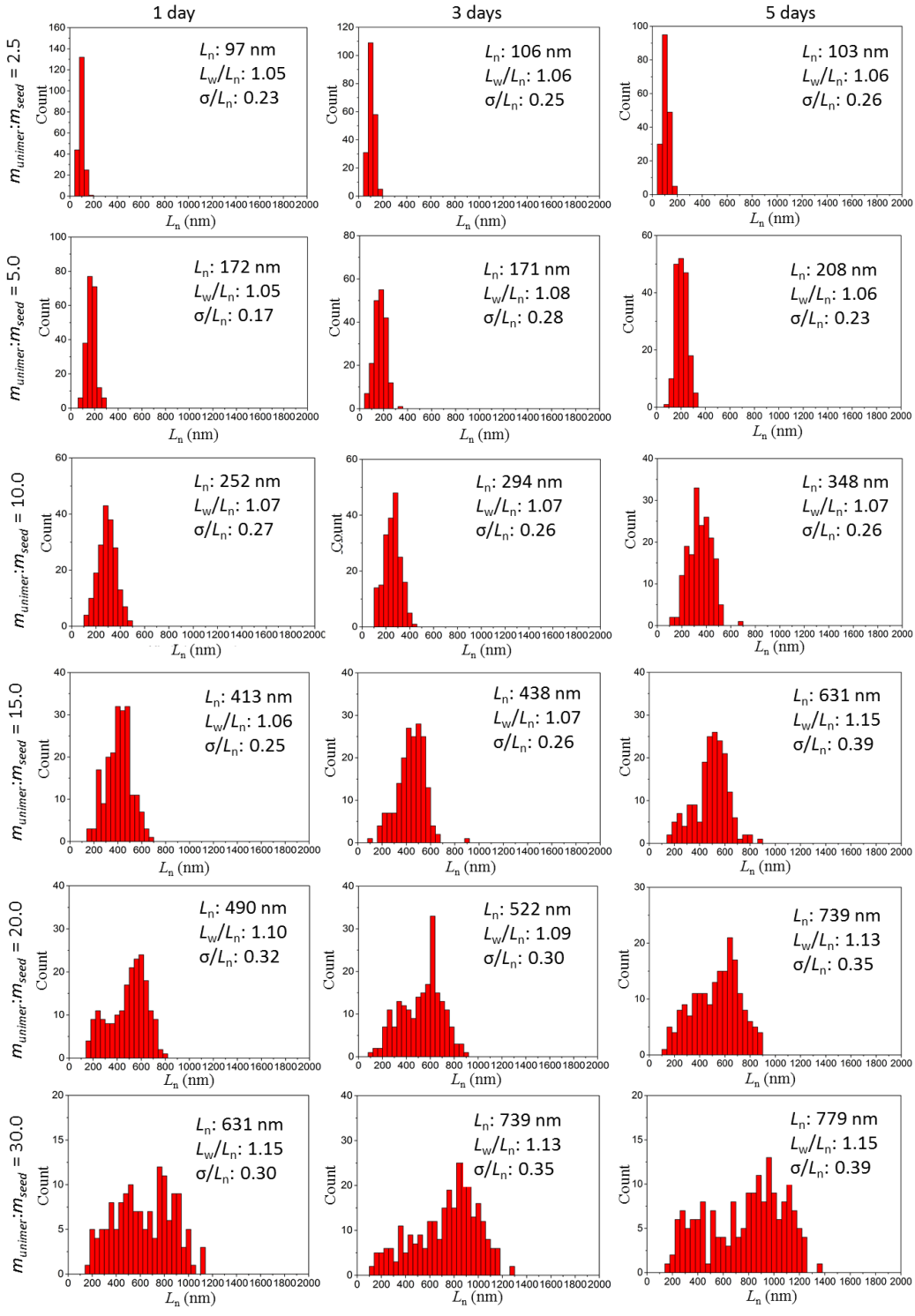

2

3 **Figure S13.** Contour length histagrams of elongated $PLLA_{47}$-*b*-$PNIPAm_{267}$ micelles in kinetic studies
4 prepared by seeded growth off seed micelles (L_n = 36 nm, L_w/L_n = 1.10, σ/L_n: 0.26) in EtOH after
5 addition of unimers (in DMSO) with unimer-to-seed mass ratios of 2.5, 5.0, 10.0, 15.0, 20.0 and 30.0.

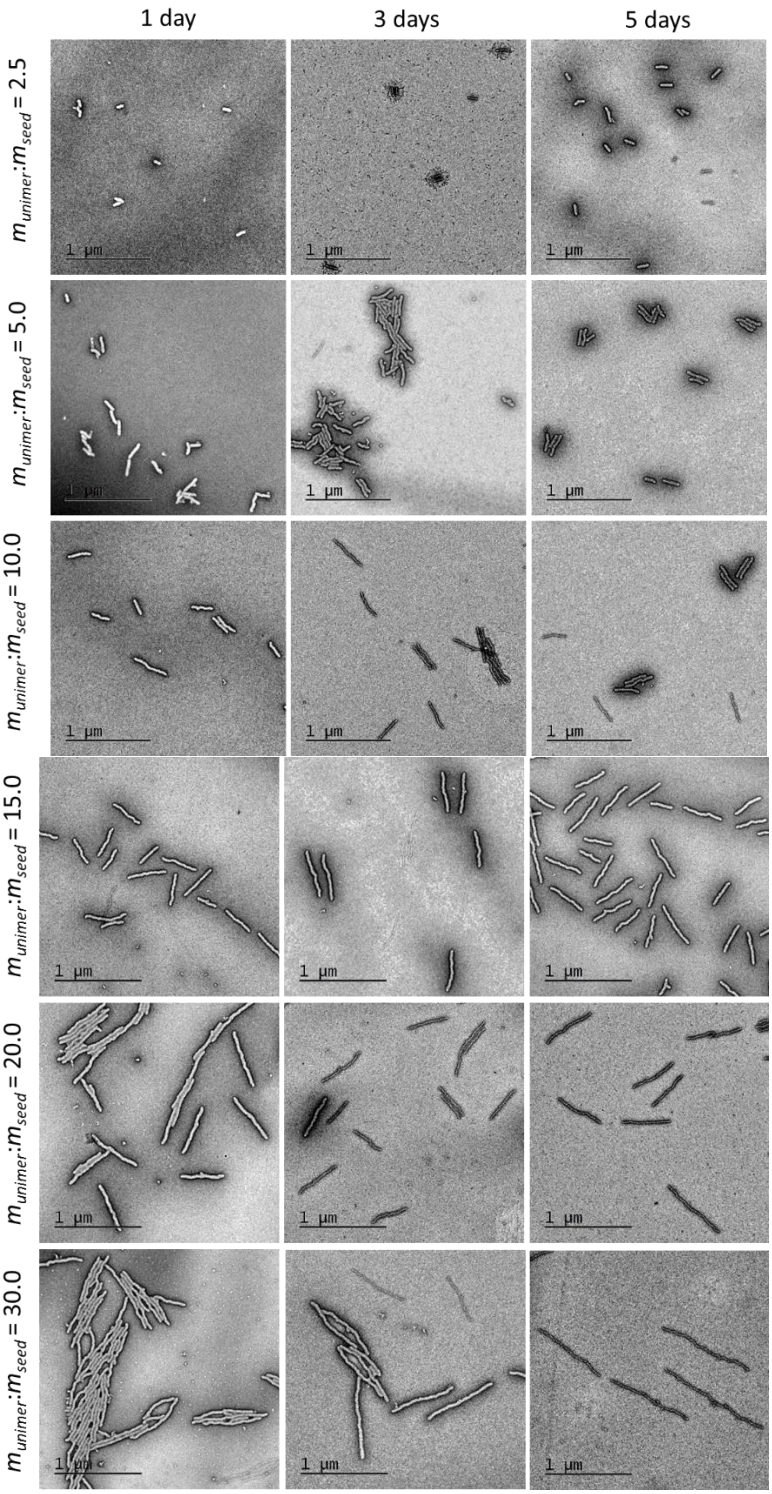

Figure S14. TEM images of uniform $PLLA_{47}$-*b*-$PNIPAm_{267}$ micelles in kinetic studies prepared by seeded growth off seed micelles (L_n = 36 nm, L_w/L_n = 1.10, σ/L_n: 0.26) in TFE/EtOH with volume ratios of 3:97, 3:97, 5:95, 8:92, 10:90 and 15:85 after addition of unimers (in DMSO) with unimer-to-seed mass ratios of 2.5, 5.0, 10.0, 15.0, 20.0 and 30.0, respectively; TEM samples were stained with a 2 wt% solution of uranyl acetate in EtOH.

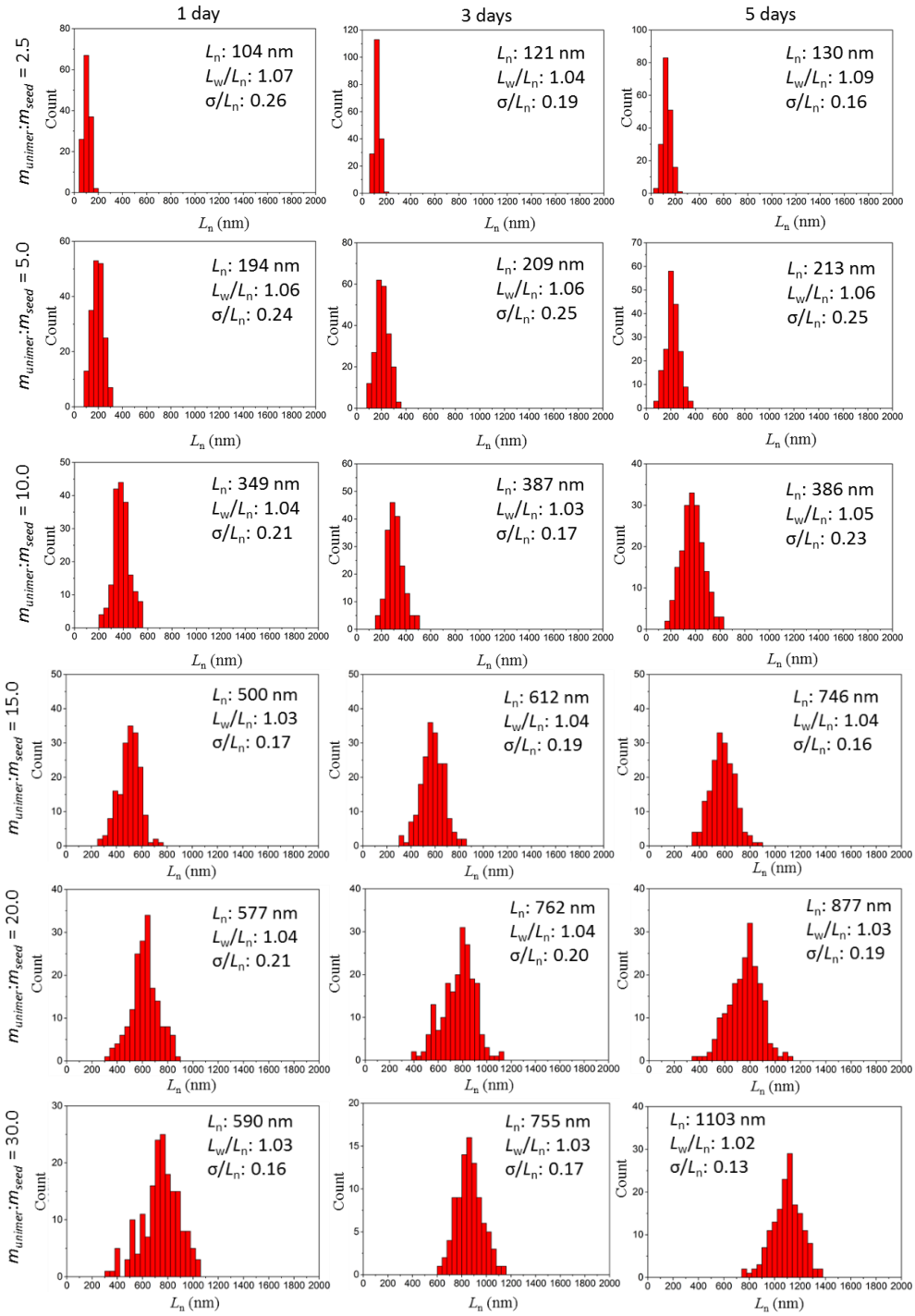

Figure S15. Contour length histagrams of uniform $PLLA_{47}$-*b*-$PNIPAm_{267}$ micelles in kinetic studies prepared by seeded growth off seed micelles (L_n = 36 nm, L_w/L_n = 1.10, σ/L_n: 0.26) in TFE/EtOH with volume ratios of 3:97, 3:97, 5:95, 8:92, 10:90 and 15:85 after addition of unimers (in DMSO) with unimer-to-seed mass ratios of 2.5, 5.0, 10.0, 15.0, 20.0 and 30.0, respectively.

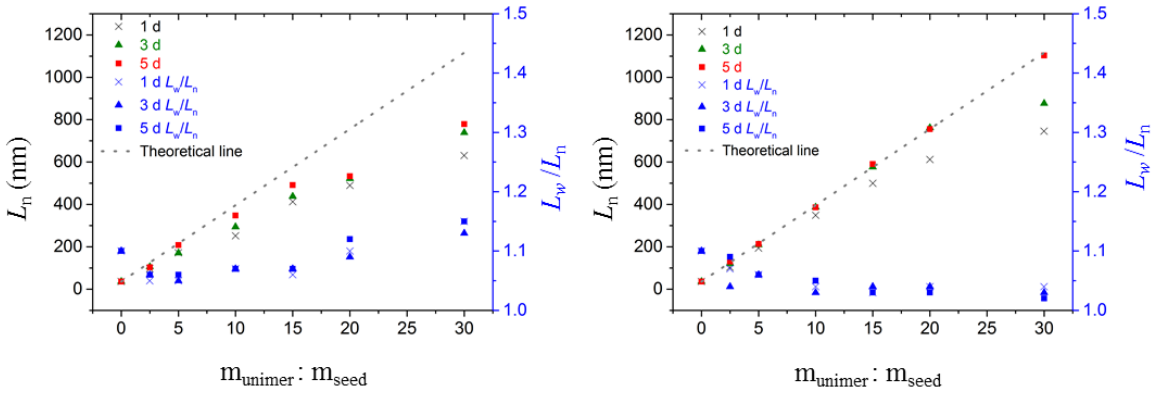

Figure S16. Plots of micelle lengths as a function of time monitored over 5 days. Unimers (in DMSO) was added to seed solutions (0.5 mg/mL, L_n = 36 nm) in (a) and in (b)EtOH TFE/EtOH (*v*:*v* = 3:97, 3:97, 5:95, 8:92, 10:90 and 15:85 for m_{unimer}:m_{seed} = 2.5, 5.0, 10.0, 15.0, 20.0 and 30.0, respectively). Black label - micelle average length; blue label - L_w/L_n.

Table S2. Data summary of kinetic studies on seeded-growth of $PLLA_{47}$-*b*-$PNIPAm_{267}$ micelles in EtOH over 5 days.

In EtOH		m_{unimer}:m_{seed}						
		0 (seed)	2.5	5.0	10.0	15.0	20.0	30.0
1 d	L_n	36	97	172	252	413	490	631
	L_w	40	102	180	271	439	540	728
	L_w/L_n	1.1	1.05	1.05	1.07	1.06	1.10	1.15
	σ	9.4	22.5	36.7	68.2	104.7	157.2	246.6
	L_n/eq	-	27	29	23	26	23	20
	σ/L_n	0.26	0.23	0.17	0.27	0.25	0.32	0.39
3 d	L_n	36	106	171	294	438	522	739
	L_w	40	113	184	300	468	570	830
	L_w/L_n	1.1	1.06	1.08	1.07	1.07	1.09	1.13
	σ	9.4	26.7	48.2	75.9	113.8	155.8	258.5
	L_n/eq	-	30	28	27	27	25	24
	σ/L_n	0.26	0.25	0.28	0.26	0.26	0.30	0.35
5 d	L_n	36	103	208	348	491	533	779
	L_w	40	109	221	373	527	596	899
	L_w/L_n	1.1	1.06	1.06	1.07	1.07	1.12	1.15
	σ	9.4	26.6	47.9	92.2	133.9	183.5	304.1
	L_n/eq	-	29	35	32	31	25	26
	σ/L_n	0.26	0.26	0.23	0.26	0.27	0.34	0.39

Table S3. Data summary of kinetic studies over 5 days on seeded-growth of $PLLA_{47}$-*b*-$PNIPAm_{267}$ micelles in TFE/EtOH with volume ratios of 3:97, 3:97, 5:95, 8:92, 10:90 and 15:85 after the addition of unimers (in DMSO) with unimer-to-seed mass ratios of 2.5, 5.0, 10.0, 15.0, 20.0 and 30.0, respectively.

In TFE/EtOH		m_{unimer}:m_{seed}						
		0 (seed)	2.5	5.0	10.0	15.0	20.0	30.0
1 d	L_n	36	104	194	349	500	612	746
	L_w	40	111	205	365	515	636	778
	L_w/L_n	1.1	1.07	1.06	1.04	1.03	1.04	1.04
	σ	9.4	27.3	47.5	73.6	85.1	120.4	155.3
	L_n/eq	-	30	32	31	31	29	24
	σ/L_n	0.26	0.26	0.24	0.21	0.17	0.19	0.16
3 d	L_n	36	121	209	387	577	762	877
	L_w	40	125	222	399	600	795	908
	L_w/L_n	1.1	1.04	1.06	1.03	1.04	1.04	1.03
	σ	9.4	22.5	51.8	67.6	122.7	157.9	165.1
	L_n/eq	-	34	34	35	36	36	28
	σ/L_n	0.26	0.19	0.25	0.17	0.21	0.20	0.19
5 d	L_n	36	130	213	386	590	755	1103
	L_w	40	142	228	406	606	779	1122
	L_w/L_n	1.1	1.09	1.06	1.05	1.03	1.03	1.02
	σ	9.4	20.4	55.1	90.1	95.7	133.6	138.2
	L_n/eq	-	37	36	35	37	36	35
	σ/L_n	0.26	0.16	0.25	0.23	0.16	0.17	0.13

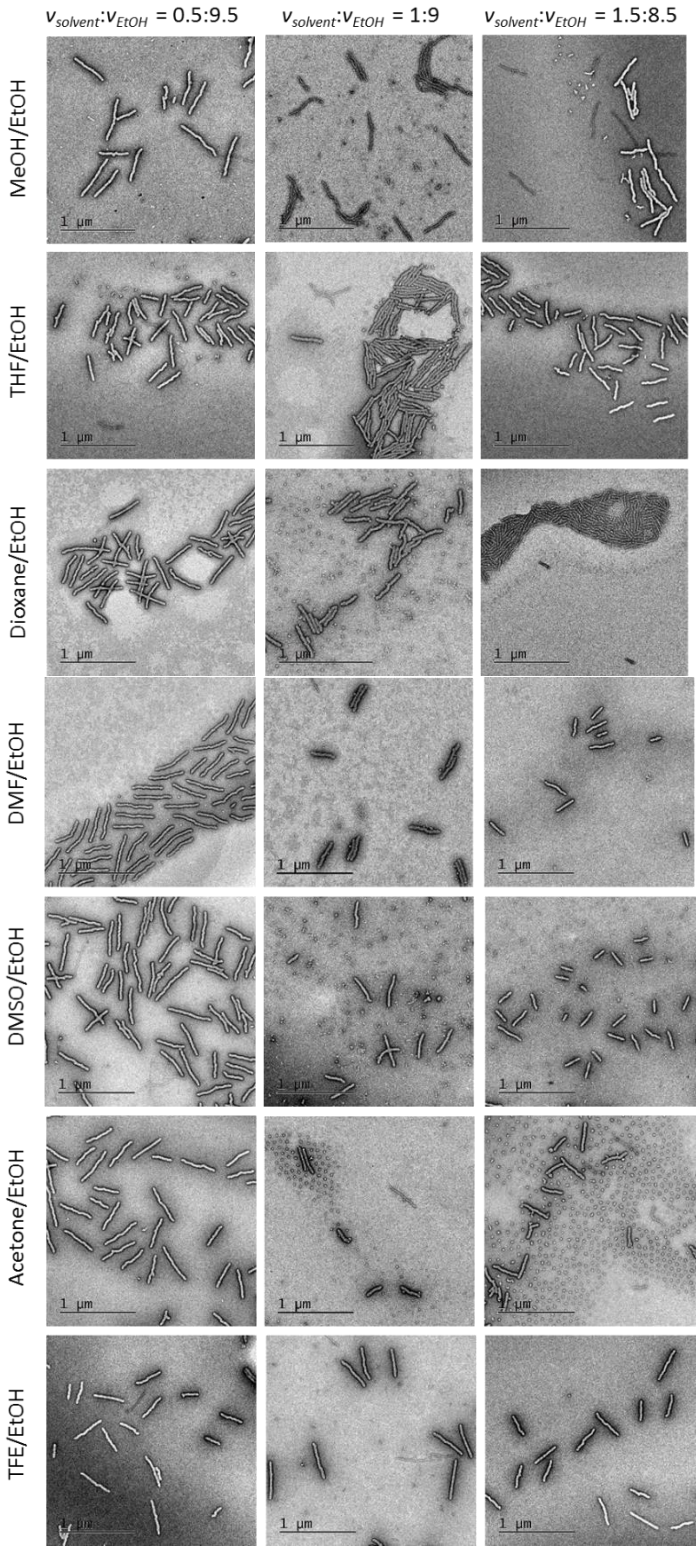

Figure S17. TEM images of uniform $PLLA_{47}$-*b*-$PNIPAm_{267}$ micelles in solvent effect studies prepared by adding unimers (m_{unimer}:m_{seed} = 15.0, in DMSO) to seed micelles (L_n = 36 nm, L_w/L_n = 1.10, σ/L_n: 0.26) in TFE/EtOH (*v*:*v* = 0.5:9.5, 1.0:9.0 and 1.5:8.5); TEM samples were stained with a 2 wt% solution of uranyl acetate in EtOH. Inset: 100 nm.

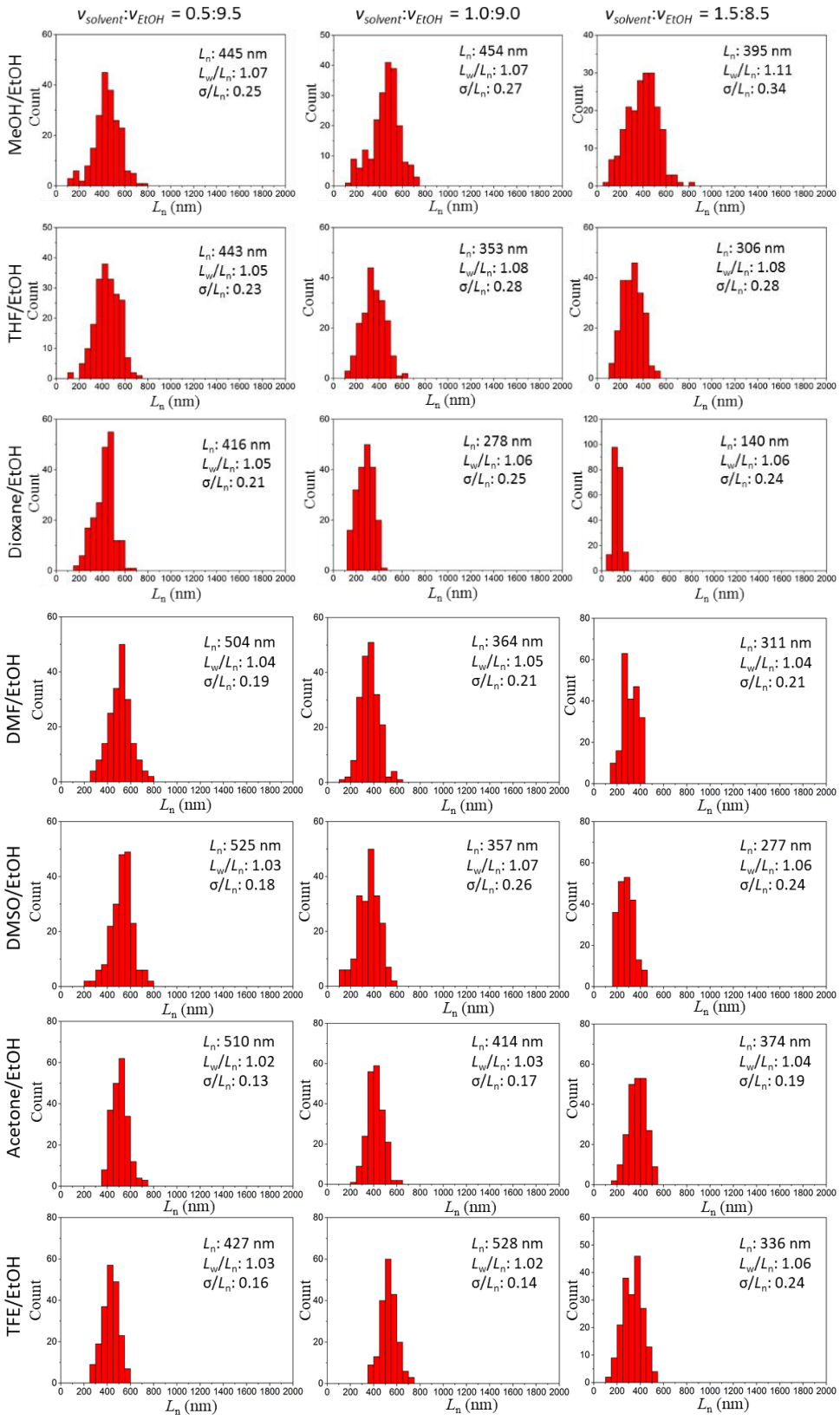

Figure S18. Contour length histograms of uniform $PLLA_{47}$-*b*-$PNIPAm_{267}$ micelles in solvent effect studies prepared by adding unimers (m_{unimer}:m_{seed} = 15.0, in DMSO) to seed micelles (L_n = 36 nm, L_w/L_n = 1.10, σ/L_n: 0.26) in TFE/EtOH (*v*:*v* = 0.5:9.5, 1.0:9.0 and 1.5:8.5).

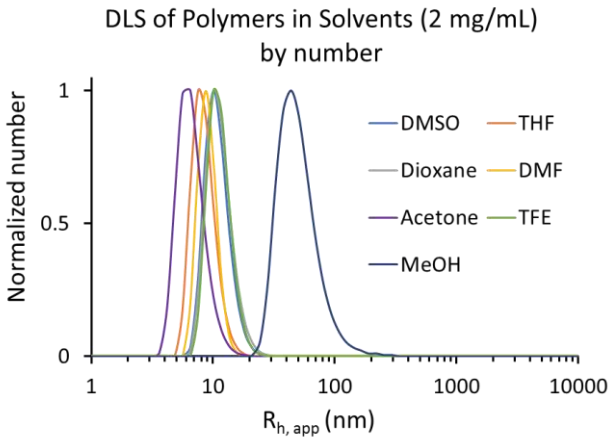

Figure S19. Solutions of $PLLA_{47}$-*b*-$PNIPAm_{267}$ in various solvents (2 mg/mL) characterized by DLS.

(a)

	$LogP_{oct}/SA$
PLLA	0.002
PNIPAm	-0.068
EtOH	-0.0002

(b)

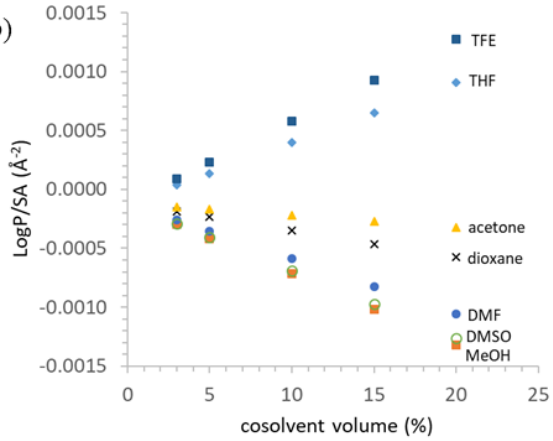

Figure S20. Calculated LogPoct/SA values of (a) PLLA, PNIPAm, EtOH and (b) solvent mixture.

Table S4. Table of Dimroth and Reichardt's Transition Energy ($E_T(30)$) of Cosolvents.

Solvents	$E_T(30)$	π*	α	β
H_2O*	62.3	1.09	1.17	0.47
TFE	61.2	0.73	1.49	0.00
DMSO	44.8	1	0.00	0.76
DMF	43.1	0.88	0.00	0.69
Acetone	41.6	0.71	0.08	0.48
THF	38.9	0.58	0.00	0.55
1,4-Dioxane	38.1	0.55	0.00	0.37
MeOH	53.6	0.60	0.98	0.66
n-Pentane*	30.2	0.00	0.00	0.00

α: scale of hydrogen bonding donor acidity
β: scale of hydrogen bonding acceptor basicity
π*: solvatochromic parameter
E_T: Dimroth and Reicharsdt's Transition Energy, a re-examined data from $E_T(30)_0$
$E_T(30) = E_T(30)_0 + s(\pi^* + d\delta) + a\alpha + b\beta$
* Scale reference of E_T

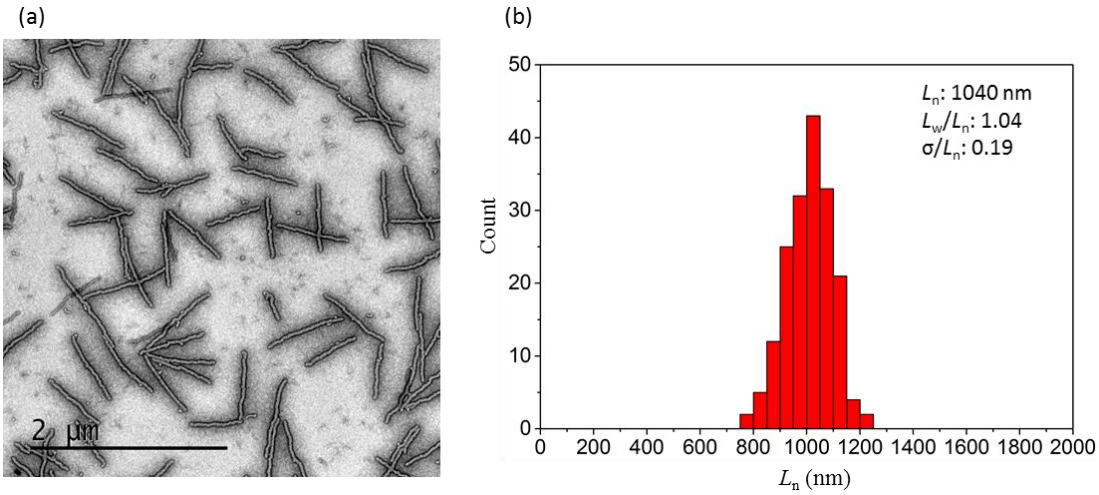

Figure S21. (a) TEM images of PLLA$_{47}$-*b*-PNIPAm$_{267}$ micelles prepared for characterization experiments with length of L_n= 1040 nm (L_w/L_n=1.04); (b) contour length histogram of measured length data. TEM image was stained with uranyl acetate solution (2% in EtOH).

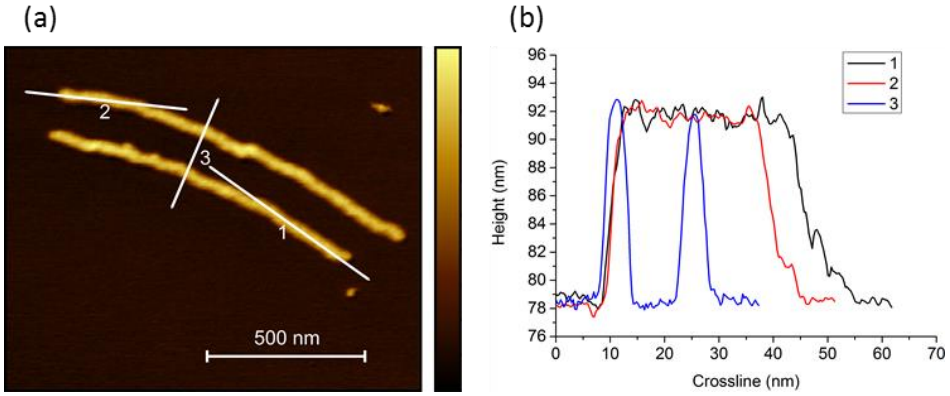

Figure S22. AFM images of PLLA$_{47}$-b-PNIPAm$_{267}$ micelles with controlled length. (a) Height image of micelles; (b) height profile by crossline measurements.

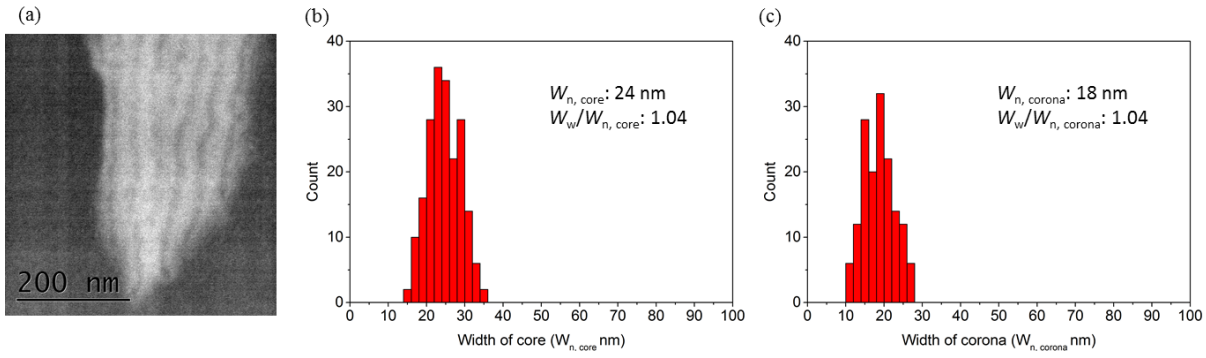

Figure S23. (a) STEM images of PLLA$_{47}$-b-PNIPAm$_{267}$ micelles in dark-field (white area is corona while dark area is core), (b) contour width histograms of core width measurement, and (c) contour width histograms of corona width measurement.

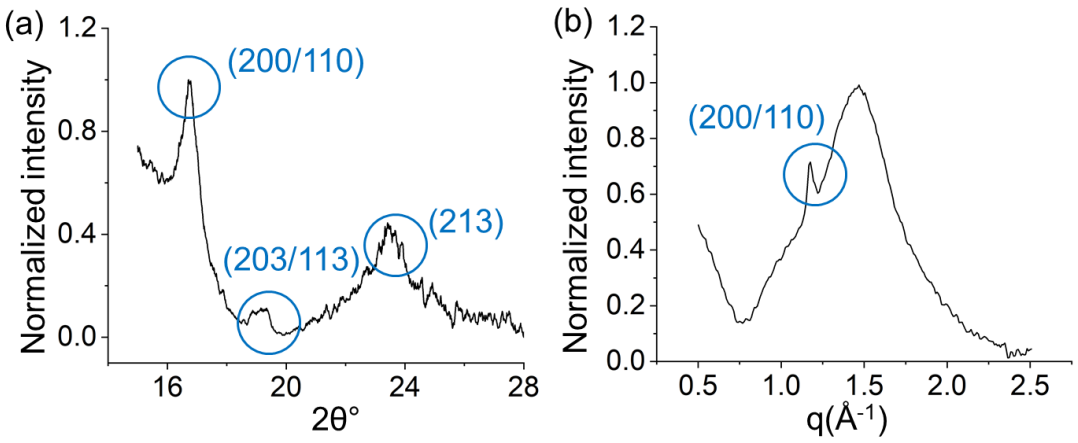

Figure S24. (a) PXRD profile of $PLLA_{47}$-*b*-$PNIPAm_{267}$ micelles; (b) normalized intensity by WAXS for $PLLA_{47}$-*b*-$PNIPAm_{267}$ micelles in EtOH with 30 mg/mL. The blue circles identify the Bragg peaks.

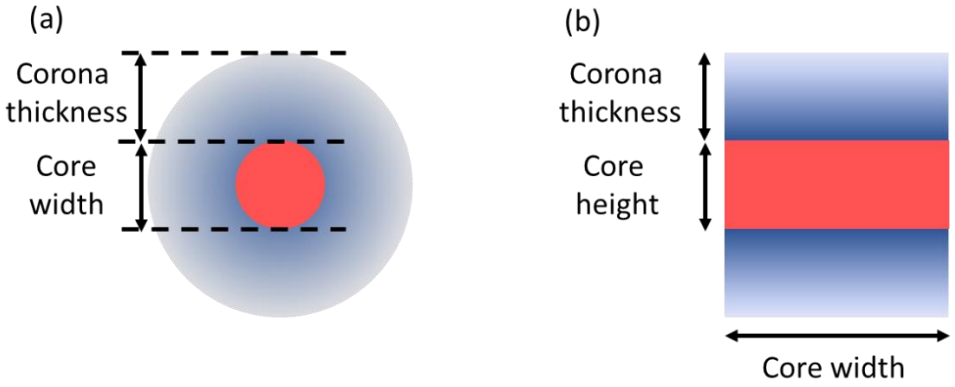

Figure S25. Schematic representation of the models used to fit SAXS data. (a) Model 1 has a homogeneous circular cross-section core (red) and a surrounding corona (blue) with decaying density; (b) Model 2 has a homogeneous rectangular cross-section core (red) with a decaying density corona (blue) attached on the long core edges.

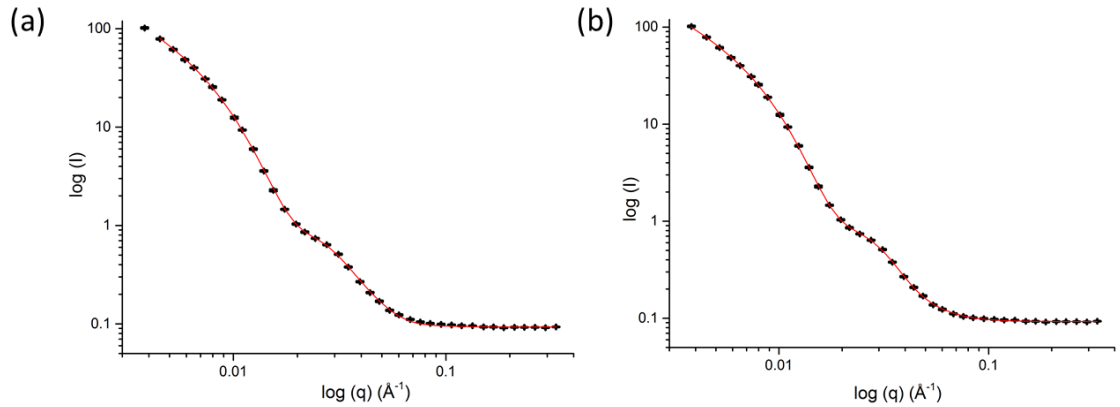

Figure S26. Plot of log (I) vs log (*q*) from SAXS data of a 4 mg/mL suspension of $PLLA_{47}$-*b*-$PNIPAm_{267}$ micelles (black in a and b) and fitting from Model 1 (red in a) and Model 2 (red in b)

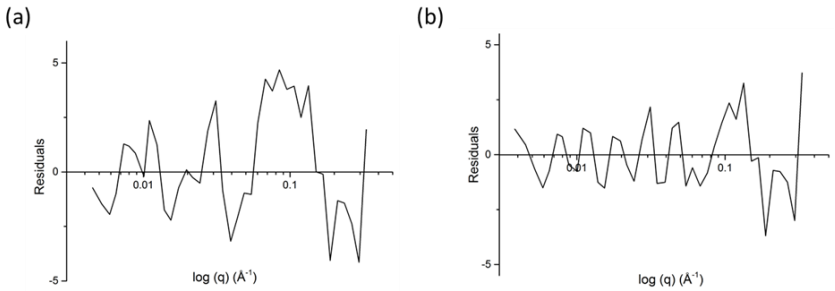

Figure S27. Plot of residual vs log (q) from Model 1 fitting data (a) and Model 2 fitting data (b).

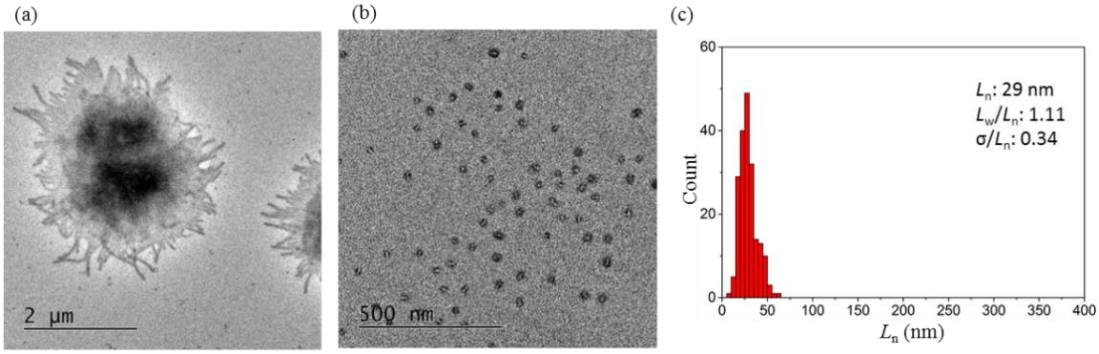

Figure S28. (a) Polydisperse $PLLA_{47}$-*b*-$P2VP_{503}$ micelles in DMSO/EtOH (1:9) with a concentration of 0.5 mg/ml prepared by heating the polymer in DMSO/EtOH (1:9) at 70 °C for 2 h followed by slow cooling over 2.5 h; (b) seeds prepared by sonication of polydisperse micelles at 0 °C for 2 h in a sonic cleaning bath; (c) contour length histogram of measured seeds length, L_n = 36 nm, L_w/L_n = 1.10.

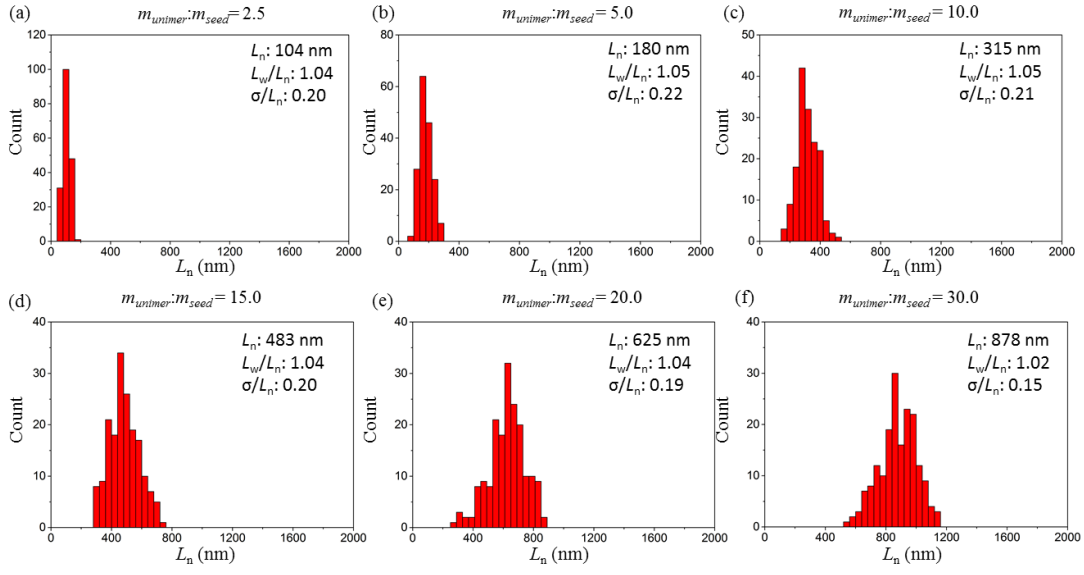

Figure S29. Contour length histogram of 5 days aged uniform $PLLA_{47}$-*b*-$P2VP_{503}$ micelles prepared by seeded growth off seed micelles (L_n = 29 nm, L_w/L_n = 1.11, σ/L_n: 0.34) in TFE/EtOH with volume ratios of (a) 3:97, (b) 3:97, (c) 5:95, (d) 8:92, (e) 10:90 and (f) 15:85 after the addition of unimers (in

DMSO) with unimer-to-seed mass ratios of (a) 2.5, (b) 5.0, (c) 10.0, (d) 15.0, (e) 20.0 and (f) 30.0, respectively.

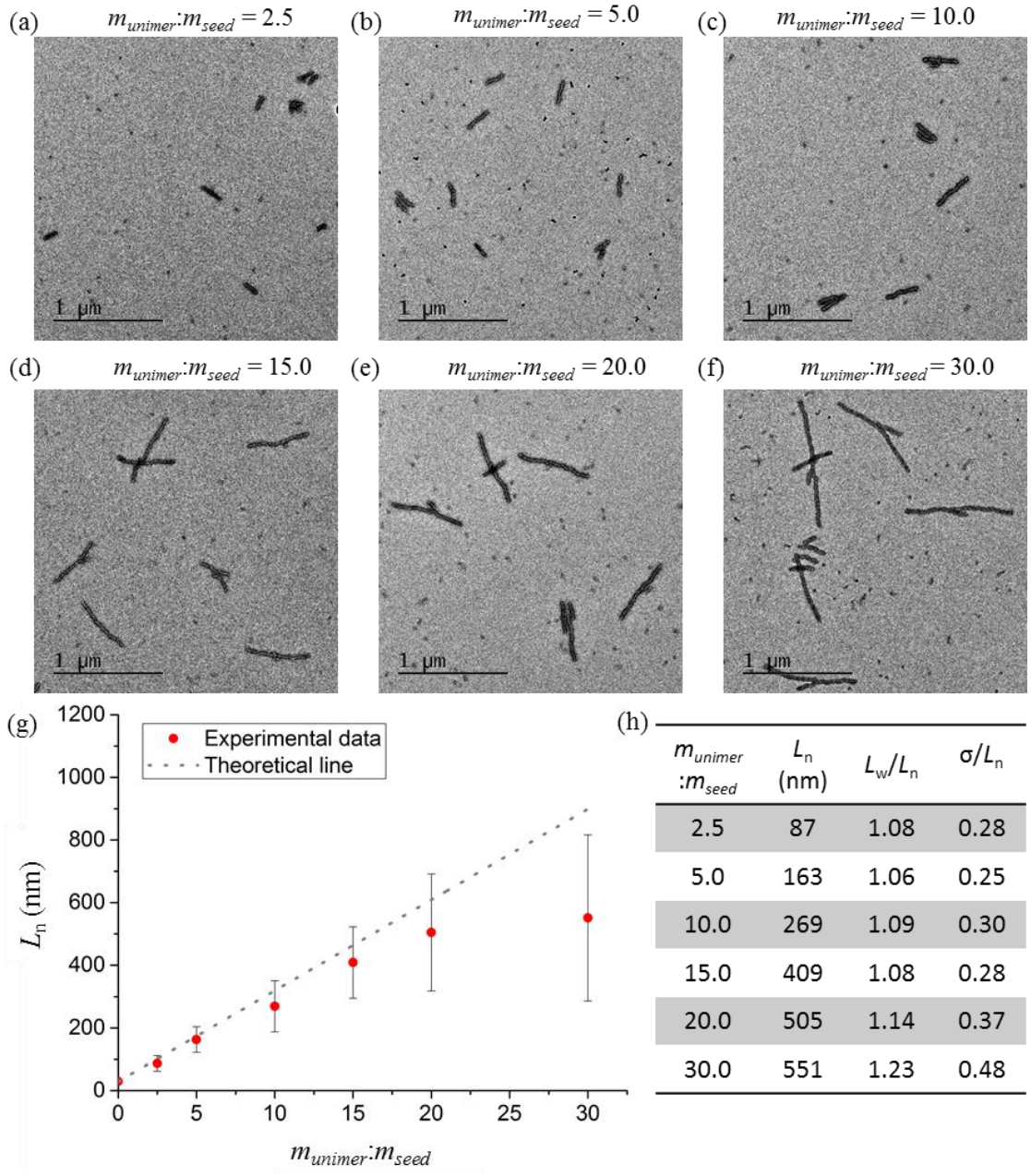

(h)

m_{unimer} :m_{seed}	L_n (nm)	L_w/L_n	σ/L_n
2.5	87	1.08	0.28
5.0	163	1.06	0.25
10.0	269	1.09	0.30
15.0	409	1.08	0.28
20.0	505	1.14	0.37
30.0	551	1.23	0.48

Figure S30. TEM images of 5 days aged samples of uniform $PLLA_{47}$-*b*-$P2VP_{503}$ micelles prepared by seeded growth off seed micelles (L_n = 29 nm, L_w/L_n = 1.11, σ/L_n: 0.34) in EtOH after the addition of unimers (in DMSO) with unimer-to-seed mass ratios of (a) 2.5, (b) 5.0, (c) 10.0, (d) 15.0, (e) 20.0 and (f) 30.0; (g) plot of number average micelle length vs m_{unimer}:m_{seed} (the error bars represent the standard deviation); (h) summary of measured length and solvent compositions; error bars were based on standard deviation.

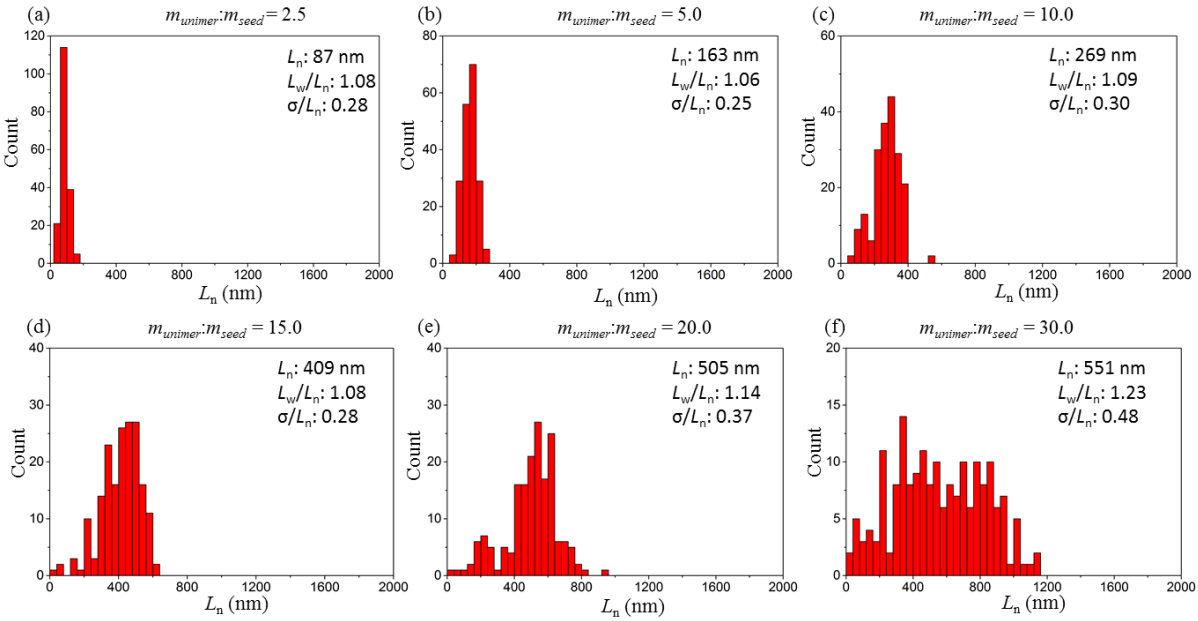

Figure S31. Contour length histogram of 5 days aged uniform $PLLA_{47}$-*b*-$P2VP_{503}$ micelles prepared by seeded growth off seed micelles (L_n = 29 nm, L_w/L_n = 1.11, σ/L_n: 0.34) in EtOH after the addition of unimers (in DMSO) with unimer-to-seed mass ratios of (a) 2.5, (b) 5.0, (c) 10.0, (d) 15.0, (e) 20.0 and (f) 30.0.

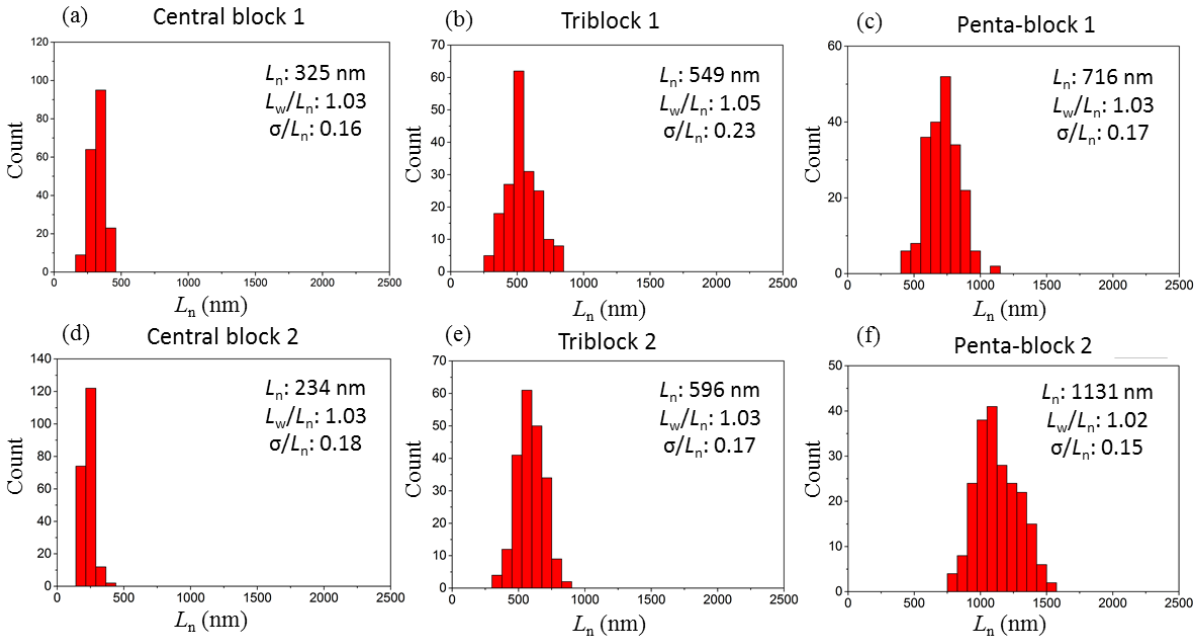

Figure S32. Contour length histograms of prepared block co-micelles: (a) central block 1, (b) triblock co-micelles 1, (c) pentablock co-micelles 1, (d) central block 2, (e) triblock co-micelles 2 and (f) pentablock co-micelles 2.

Formula for SAXS Data Fitting with Model 2

Model 2 (Figure S33)describes a long rigid micelle with a rectangular cross-section (2*a* by 2*b*) core covered by corona on two faces perpendicular to the *a* direction. The core has a uniform scattering length density, ρ_{core}. The coronas have a rectangular cross-section (2*b* by *c*) with a linear decaying scattering intensity from the inner, ρ_{in}, to outer side, ρ_{out}. For the fitting process, the long rods approximation is used by considering the micelle length (2*l*) is significantly greater than the reciprocal of the minimum *q*. The scattering intensity (I(*q*)) from long rods solution can be described as:

$$I(q) = \frac{2\pi l}{q}\langle F_a(Qsin\phi)F_{bd}(qcos\phi)\rangle_\phi$$

where the angle brackets represent an average over the azimuthal angle of *q* with respect to the long micelle axis. The structure factors for the cross-section are defined as follows:

$$F_b(q) = 2bsinc(qb)$$

$$F_a(q) = 2\sum_{j=1,N}(\rho_j + \rho_{j+1})d_j sinc(qd_j)$$

where $\rho_j = \rho_{core}$ for $j = 1$, $\rho_j = \rho_{solvent}$ for $j = 1 + N$, and $\rho_j = \rho_{in} + (\rho_{out} - \rho_{in})[(j - 1.5)/(N - 1)]$ otherwise, while $d_j = a$ for $j = 1$ and $d_j = a + c(j - 1)/(N - 1)$ otherwise. The three dimensions, *a*, *b*, and *c* were assumed to have Schultz distributions and the expression was averaged numerically over these distributions.

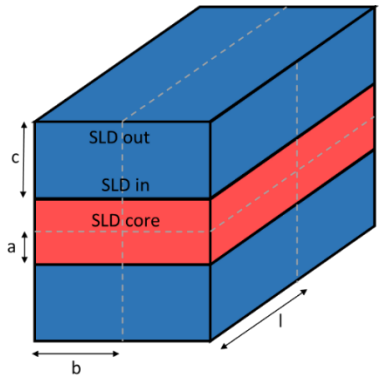

Figure S33. Schematic representation of Model 2 used in SAXS data fitting. Distances *a*, *b*, *c* and *l* represent half the core thickness, half the micelle width, the corona thickness and the micelle length respectively. SLD = scattering length density.

Supporting Information References

1. Inam, M.; Cambridge, G.; Pitto-Barry, A.; Laker, Z. P. L.; Wilson, N. R.; Mathers, R. T.; Dove, A. P.; O'Reilly, R. K., 1D vs. 2D shape selectivity in the crystallization-driven self-assembly of polylactide block copolymers. *Chem Sci* **2017,** *8* (6), 4223-4230.
2. Jones, E. R.; Semsarilar, M.; Blanazs, A.; Armes, S. P., Efficient Synthesis of Amine-Functional Diblock Copolymer Nanoparticles via RAFT Dispersion Polymerization of Benzyl Methacrylate in Alcoholic Media. *Macromolecules* **2012,** *45* (12), 5091-5098.
3. Skey, J.; O'Reilly, R. K., Facile one pot synthesis of a range of reversible addition-fragmentation chain transfer (RAFT) agents. *Chem Commun (Camb)* **2008,** (35), 4183-5.
4. Boott, C. E.; Leitao, E. M.; Hayward, D. W.; Laine, R. F.; Mahou, P.; Guerin, G.; Winnik, M. A.; Richardson, R. M.; Kaminski, C. F.; Whittell, G. R.; Manners, I., Probing the Growth Kinetics for the Formation of Uniform 1D Block Copolymer Nanoparticles by Living Crystallization-Driven Self-Assembly. *ACS Nano* **2018,** *12* (9), 8920-8933.
5. Finnegan, J. R.; Lunn, D. J.; Gould, O. E.; Hudson, Z. M.; Whittell, G. R.; Winnik, M. A.; Manners, I., Gradient crystallization-driven self-assembly: cylindrical micelles with "patchy" segmented coronas via the coassembly of linear and brush block copolymers. *J Am Chem Soc* **2014,** *136* (39), 13835-44.
6. Xu, J.; Zhou, H.; Yu, Q.; Manners, I.; Winnik, M. A., Competitive Self-Assembly Kinetics as a Route To Control the Morphology of Core-Crystalline Cylindrical Micelles. *J Am Chem Soc* **2018,** *140* (7), 2619-2628.
7. Mencer, H. J.; Grubisic-gallot, Z., Influence of Solvent Polarity on Elution Volume in the Case of Polar Polymers. *Journal of Liquid Chromatography* **1979,** *2* (5), 649-662.